Supporting Information for

Synthesis, Characterization, and Reactivity of Iron(III) Complexes Supported by a Trianionic ONO^{3-} Pincer Ligand

*Matias E. Pascualini,[≠¶] Natali V. Di Russo,[≠] Pedro A. Quintero,[a] Annaliese A. Thuijs,[≠¶] Dawid Pinkowicz,[†#] Khalil A. Abboud,[≠¶] Kim R. Dunbar,[†] George Christou,[≠¶] Mark W. Meisel,[a] and Adam S. Veige[≠¶]**

[≠] Department of Chemistry, [¶]Center for Catalysis, and [a]Department of Physics, University of Florida. Gainesville, FL 32611, United States.

[†]Department of Chemistry, Texas A&M University. College Station, TX 77842-3012, United States.

[#]Faculty of Chemistry, Jagiellonian University, Ingardena 3, 30-060 Kraków, Poland.

Table of Contents

1. General Considerations.

Unless specified otherwise, all manipulations were performed under an inert atmosphere using standard Schlenk or glovebox techniques. Glassware was oven dried before use. Pentane, toluene, tetrahydrofuran (THF), 1,2-dimethoxyethane (DME) were dried using a GlassContours drying column. Benzene-d_6 (Cambridge Isotopes) was dried over sodium-benzophenone ketyl and distilled or vacuum transferred and stored over 4 Å molecular sieves. $FeCl_3$ 98% (anhydrous) was purchased from Acros Organics, and used as received.

NMR spectra were obtained on Varian Mercury Broad Band 300 MHz, or Varian Mercury 300 MHz spectrometers. Chemical shifts are reported in δ (ppm). For ^1H NMR spectra the solvent resonance was referenced as an internal reference. The baseline was corrected manually. Elemental analyses were performed at Complete Analysis Laboratory Inc., Parsippany, New Jersey.

EPR measurements were conducted using a Bruker Elexsys-500 spectrometer at the X-band microwave frequency at ~9.6 Ghz at 10 K. The microwave frequency was measured with a built-in digital counter, and the magnetic field was calibrated using 2,2-diphenyl-1-picrylhydrazyl (DPPH; g = 2.0037). The temperature was controlled using an Oxford Instruments cryostat, to accuracy within $\pm$ 0.1 K. Modulation amplitude and microwave power were optimized for high signal-to-noise ratio and narrow peaks.

Cyclic voltammetry was performed under a nitrogen atmosphere using a standard three-electrode setup. A glassy carbon electrode (3 mm diameter) was used as a

working electrode, a platinum wire as counter electrode, and Ag/AgCl as reference electrode. The measurements were made in 0.1 M Bu_4NPF_6 acetonitrile solution, and a 10 mM ferrocene solution was used as external reference. Bu_4NPF_6 99.0% was purchased from Sigma-Aldrich, and used as received. Electrodes were purchased from either BASi, Inc. or CH Instruments, Inc. Potential sweeps were controlled by a Princeton Applied Research Versastat II potentiostat.

Variable-temperature dc and ac magnetic susceptibility data was collected in the 2.0 – 300.0 K range using a Quantum Design MPMS-XL SQUID magnetometer equipped with a 7 T dc magnet in an applied field of 100 G. The microcrystalline samples were restrained in eicosane to prevent torquing. Diamagnetic corrections using Pascal's constants were applied to the observed susceptibilities to obtain the molar paramagnetic susceptibility (χ_M).

2. X-ray crystallography of 1

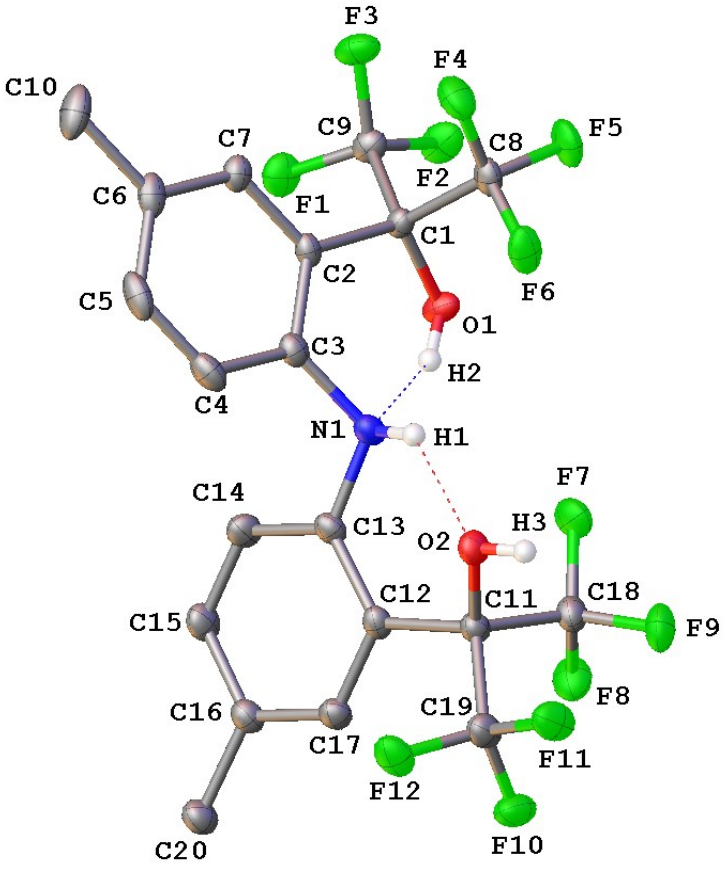

Figure S1. Molecular structure of **1**. Ellipsoids drawn at the 50 % probability level. Arene and methyl group hydrogen atoms and solvent molecules were removed for clarity.

X-ray Experimental for 1.

X-Ray Intensity data were collected at 100 K on a Bruker **DUO** diffractometer using MoKα radiation (λ = 0.71073 Å) and an APEXII CCD area detector.

Raw data frames were read by program SAINT and integrated using 3D profiling algorithms. The resulting data were reduced to produce hkl reflections and their intensities and estimated standard deviations. The data were corrected for Lorentz and polarization effects and numerical absorption corrections were applied based on indexed and measured faces.

The structure was solved and refined in SHELXTL6.1, using full-matrix least-squares refinement. The non-H atoms were refined with anisotropic thermal parameters and all of the H atoms were calculated in idealized positions and refined riding on their parent atoms. In addition to the molecules, the asymmetric unit contains a half pentane solvent molecule located on an inversion center. Both hydroxyl protons and the hydrogen on N1 were obtained from a Difference Fourier map and refined freely. All three protons are involved in intra and intermolecular hydrogen bonding. In the final cycle of refinement, 31270 reflections (of which 4539 are observed with $I > 2\sigma(I)$) were used to refine 352 parameters and the resulting R_1, wR_2 and S (goodness of fit) were 3.48%, 8.77% and 0.941, respectively. The refinement was carried out by minimizing the wR_2 function using F^2 rather than F values. R_1 is calculated to provide a reference to the conventional R value but its function is not minimized.

Table S1. Crystal data and structure refinement for 1.

Identification code	pasc15	
Empirical formula	$C_{22.50}H_{18}F_{12}NO_2$	
Formula weight	562.38	
Temperature	100(2) K	
Wavelength	0.71073 Å	
Crystal system	Monoclinic	
Space group	$P2_1/n$	
Unit cell dimensions	a = 11.3214(5) Å	α = 90°.
	b = 18.4917(8) Å	β = 111.883(1)°.
	c = 11.9749(5) Å	γ = 90°.
Volume	2326.33(17) $Å^3$	
Z	4	
Density (calculated)	1.606 Mg/m^3	
Absorption coefficient	0.167 mm^{-1}	
F(000)	1136	
Crystal size	0.37 x 0.11 x 0.11 mm^3	
Theta range for data collection	2.11 to 27.50°.	
Index ranges	-14≤h≤14, -24≤k≤24, -15≤l≤12	
Reflections collected	31270	
Independent reflections	5291 [R(int) = 0.0187]	
Completeness to theta = 27.50°	99.2 %	
Absorption correction	Integration	
Max. and min. transmission	0.9825 and 0.9407	
Refinement method	Full-matrix least-squares on F^2	
Data / restraints / parameters	5291 / 0 / 352	
Goodness-of-fit on F^2	0.941	
Final R indices [I>2sigma(I)]	R1 = 0.0348, wR2 = 0.0877 [4539]	
R indices (all data)	R1 = 0.0426, wR2 = 0.0930	
Largest diff. peak and hole	0.446 and -0.227 $e.Å^{-3}$	

$R1 = \Sigma(||F_o| - |F_c||) / \Sigma|F_o|$

$wR2 = [\Sigma[w(F_o^2 - F_c^2)^2] / \Sigma[w(F_o^2)^2]]^{1/2}$

$S = [\Sigma[w(F_o^2 - F_c^2)^2] / (n-p)]^{1/2}$

$w= 1/[\sigma^2(F_o^2)+(m*p)^2+n*p]$, $p = [\max(F_o^2,0)+ 2* F_c^2]/3$, m & n are constants.

Table S2. Atomic coordinates (x 10^4) and equivalent isotropic dispacement parameters ($Å^2$x 10^3) for **1**. U(eq) is defined as one third of the trace of the orthogonalized U^{ij} tensor.

Atom	x	y	Z	U(eq)
F1	5452(1)	4053(1)	-2931(1)	28(1)
F2	5671(1)	2957(1)	-3404(1)	29(1)
F3	6913(1)	3780(1)	-3607(1)	28(1)
F4	9159(1)	3338(1)	-1970(1)	30(1)
F5	8029(1)	2374(1)	-2272(1)	31(1)
F6	9052(1)	2745(1)	-465(1)	31(1)
F7	7547(1)	2035(1)	1574(1)	29(1)
F8	6665(1)	1829(1)	2853(1)	31(1)
F9	8598(1)	1487(1)	3236(1)	32(1)
F10	7961(1)	2327(1)	5109(1)	32(1)
F11	9866(1)	2358(1)	5133(1)	32(1)
F12	8926(1)	3347(1)	5231(1)	30(1)
O1	6505(1)	2971(1)	-1122(1)	21(1)
O2	9303(1)	2960(1)	3032(1)	20(1)
N1	7647(1)	3556(1)	970(1)	19(1)
C1	7222(1)	3408(1)	-1591(1)	16(1)
C2	7705(1)	4112(1)	-884(1)	16(1)
C3	7867(1)	4172(1)	327(1)	18(1)
C4	8283(1)	4827(1)	930(1)	24(1)
C5	8548(1)	5409(1)	351(2)	26(1)
C6	8436(1)	5358(1)	-842(1)	22(1)
C7	8025(1)	4707(1)	-1441(1)	18(1)
C8	8378(1)	2963(1)	-1588(1)	21(1)
C9	6309(1)	3554(1)	-2900(1)	20(1)
C10	8743(2)	5995(1)	-1467(2)	32(1)
C11	8253(1)	2761(1)	3321(1)	18(1)
C12	7184(1)	3321(1)	2817(1)	18(1)
C13	6946(1)	3684(1)	1724(1)	18(1)
C14	5913(1)	4160(1)	1300(1)	23(1)
C15	5151(1)	4296(1)	1941(1)	23(1)
C16	5376(1)	3952(1)	3034(1)	21(1)
C17	6373(1)	3458(1)	3434(1)	20(1)
C18	7755(1)	2016(1)	2748(1)	23(1)
C19	8743(1)	2698(1)	4716(1)	24(1)
C20	4603(1)	4128(1)	3784(1)	24(1)
C21	2229(4)	4528(2)	4978(4)	37(1)
C22	1389(3)	4763(2)	5653(3)	28(1)
C23	40(3)	4917(2)	4821(3)	25(1)
C24	-805(3)	5156(2)	5496(3)	34(1)

C25	-2187(4)	5279(3)	4662(4)	46(1)

Table S3. Bond lengths (Å) for 1.

Bond	Length (Å)	Bond	Length (Å)
F1-C9	1.3288(17)	C2-C3	1.3966(19)
F2-C9	1.3345(16)	C2-C7	1.4015(19)
F3-C9	1.3385(17)	C3-C4	1.3976(19)
F4-C8	1.3307(17)	C4-C5	1.372(2)
F5-C8	1.3316(15)	C5-C6	1.389(2)
F6-C8	1.3371(17)	C6-C7	1.3904(19)
F7-C18	1.3366(17)	C6-C10	1.504(2)
F8-C18	1.3311(17)	C11-C12	1.5354(18)
F9-C18	1.3390(16)	C11-C18	1.5484(19)
F10-C19	1.3371(18)	C11-C19	1.556(2)
F11-C19	1.3374(16)	C12-C17	1.3990(19)
F12-C19	1.3306(18)	C12-C13	1.4049(19)
O1-C1	1.4019(16)	C13-C14	1.4001(19)
O1-H2	0.83(2)	C14-C15	1.376(2)
O2-C11	1.4059(16)	C15-C16	1.391(2)
O2-H3	0.80(2)	C16-C17	1.3908(19)
N1-C13	1.4256(17)	C16-C20	1.5049(19)
N1-C3	1.4480(18)	C21-C22	1.523(5)
N1-H1	0.837(19)	C22-C23	1.507(5)
C1-C2	1.5379(17)	C23-C24	1.530(4)
C1-C8	1.5459(19)	C24-C25	1.527(5)
C1-C9	1.5460(18)		

Table S4. Bond angles (°) for 1.

Bond	Angle (°)	Bond	Angle (°)
C1-O1-H2	107.7(16)	F3-C9-C1	112.94(11)
C11-O2-H3	109.0(15)	O2-C11-C12	110.00(11)
C13-N1-C3	116.90(11)	O2-C11-C18	108.99(11)
C13-N1-H1	111.6(12)	C12-C11-C18	108.83(11)
C3-N1-H1	111.8(12)	O2-C11-C19	106.72(11)
O1-C1-C2	114.07(11)	C17-C12-C11	119.37(12)
O1-C1-C8	107.96(11)	C13-C12-C11	122.50(12)
C2-C1-C8	108.77(10)	C14-C13-C12	118.82(12)
O1-C1-C9	103.82(10)	C14-C13-N1	117.50(12)
C2-C1-C9	112.13(10)	C12-C13-N1	123.53(12)
C8-C1-C9	109.93(11)	C15-C14-C13	121.72(13)
C3-C2-C7	118.33(12)	C14-C15-C16	120.57(13)
C3-C2-C1	121.40(12)	C17-C16-C15	117.71(13)
C7-C2-C1	120.25(12)	C17-C16-C20	120.96(13)
C2-C3-C4	119.56(13)	C15-C16-C20	121.29(13)
C2-C3-N1	120.50(12)	C16-C17-C12	123.03(13)
C4-C3-N1	119.90(13)	F8-C18-F7	107.42(12)
C5-C4-C3	120.90(14)	F8-C18-F9	107.68(12)
C4-C5-C6	120.84(13)	F7-C18-F9	107.17(12)
C5-C6-C7	118.28(13)	F8-C18-C11	112.77(11)
C5-C6-C10	120.64(13)	F7-C18-C11	109.61(11)
C7-C6-C10	121.09(14)	F9-C18-C11	111.95(12)
C6-C7-C2	122.00(13)	F12-C19-F10	108.02(12)
F4-C8-F5	107.34(12)	F12-C19-F11	106.81(12)
F4-C8-F6	107.42(11)	F10-C19-F11	106.79(12)
F5-C8-F6	107.39(11)	F12-C19-C11	111.22(12)
F4-C8-C1	113.13(11)	F10-C19-C11	113.50(12)
F5-C8-C1	112.14(11)	F11-C19-C11	110.19(11)
F6-C8-C1	109.16(11)	C23-C22-C21	112.4(3)
F1-C9-F2	107.18(11)	C22-C23-C24	112.6(3)
F1-C9-F3	107.80(11)	C25-C24-C23	112.8(3)
F2-C9-F3	106.79(11)	C12-C11-C19	112.71(11)
F1-C9-C1	110.81(11)	C18-C11-C19	109.52(12)
F2-C9-C1	111.04(11)	C17-C12-C13	118.07(12)

Table S5. Anisotropic displacement parameters ($Å^2 x\ 10^3$) for **1**. The anisotropic displacement factor exponent takes the form: $-2\pi^2[h^2\ a^{*2}U^{11} + ...\ + 2\ h\ k\ a^*\ b^*\ U^{12}\ ]$.

Atom	U_{11}	U_{22}	U_{33}	U_{23}	U_{13}	U_{12}
F1	21(1)	29(1)	25(1)	2(1)	-1(1)	4(1)
F2	32(1)	28(1)	18(1)	-4(1)	-1(1)	-12(1)
F3	32(1)	34(1)	16(1)	1(1)	8(1)	-8(1)
F4	24(1)	28(1)	40(1)	-8(1)	16(1)	-1(1)
F5	37(1)	20(1)	32(1)	-13(1)	7(1)	1(1)
F6	31(1)	26(1)	25(1)	-2(1)	-2(1)	11(1)
F7	39(1)	24(1)	25(1)	-9(1)	11(1)	-4(1)
F8	28(1)	26(1)	43(1)	0(1)	17(1)	-4(1)
F9	34(1)	19(1)	43(1)	2(1)	14(1)	8(1)
F10	35(1)	38(1)	26(1)	12(1)	17(1)	11(1)
F11	27(1)	43(1)	23(1)	8(1)	6(1)	18(1)
F12	33(1)	35(1)	18(1)	-5(1)	3(1)	8(1)
O1	26(1)	21(1)	16(1)	-1(1)	6(1)	-8(1)
O2	17(1)	20(1)	21(1)	2(1)	6(1)	4(1)
N1	20(1)	22(1)	15(1)	0(1)	6(1)	5(1)
C1	18(1)	14(1)	14(1)	-1(1)	4(1)	-2(1)
C2	12(1)	14(1)	17(1)	-2(1)	2(1)	2(1)
C3	15(1)	19(1)	19(1)	-2(1)	4(1)	2(1)
C4	22(1)	27(1)	23(1)	-11(1)	6(1)	0(1)
C5	19(1)	19(1)	38(1)	-14(1)	7(1)	-2(1)
C6	13(1)	16(1)	34(1)	-2(1)	4(1)	2(1)
C7	14(1)	17(1)	22(1)	0(1)	3(1)	1(1)
C8	24(1)	16(1)	20(1)	-5(1)	4(1)	1(1)
C9	22(1)	20(1)	16(1)	-1(1)	3(1)	-4(1)
C10	23(1)	16(1)	50(1)	3(1)	5(1)	-2(1)
C11	18(1)	19(1)	16(1)	0(1)	6(1)	4(1)
C12	17(1)	18(1)	15(1)	-2(1)	2(1)	3(1)
C13	18(1)	21(1)	15(1)	-4(1)	5(1)	1(1)
C14	23(1)	26(1)	16(1)	3(1)	4(1)	6(1)
C15	20(1)	26(1)	21(1)	1(1)	4(1)	8(1)
C16	19(1)	23(1)	19(1)	-3(1)	6(1)	3(1)
C17	21(1)	22(1)	15(1)	-1(1)	6(1)	2(1)
C18	24(1)	19(1)	27(1)	0(1)	11(1)	3(1)
C19	24(1)	28(1)	19(1)	3(1)	7(1)	10(1)
C20	23(1)	28(1)	23(1)	0(1)	9(1)	7(1)

Table S6. Hydrogen bonds for **1** (Å and °).

D-H...A	d(D-H)	d(H...A)	d(D...A)	<(DHA)
N1-H1...O2	0.837(19)	2.038(19)	2.7160(16)	137.6(16)
O1-H2...N1	0.83(2)	1.82(2)	2.5892(16)	153(2)
O2-H3...O1#1	0.80(2)	2.10(2)	2.8850(14)	169(2)

Symmetry transformations used to generate equivalent atoms:

#1 x+1/2,-y+1/2,z+1/2

3. Synthesis of 3.

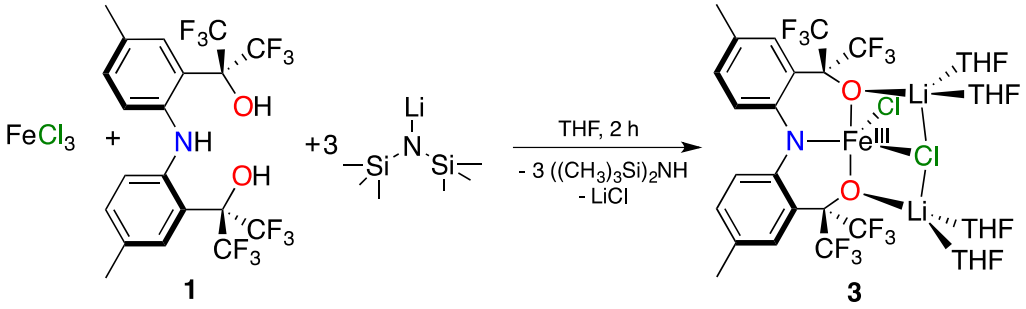

Figure S2. Synthesis of **3**.

Proligand **1** (1.000 g, 1.889 mmol) was dissolved in THF (1 mL) and three equivalents of $((CH_3)_3Si)_2NLi$, 97 % (0.978 g, 5.669 mmol) in THF (2 mL) were added dropwise to generate the trianionic $[CF_3\text{-}ONO]^{3-}$ species *in situ*. This solution was slowly added to a THF (2 mL) solution of $FeCl_3$, 98 % (0.313 g, 1.891 mmol), yielding a blue solution and a significant amount of precipitated LiCl. After stirring the solution for 2 hours at room temperature and filtering the inorganic precipitate, the solvent was evaporated under reduced pressure. The resulting blue powder was dissolved in toluene, which produced a green solution, stirred for one hour, and filtered to remove the remaining inorganic salts. The solvent was evaporated under reduced pressure. The residue was extracted with THF and an equal amount of pentane was added. Cooling this solution at -35°C overnight yielded green crystals (needle shaped) that were isolated and dried under vacuum (1.316 g, 72.9 %). ^{1}H-NMR (C_6D_6, 300 MHz, 25 °C) δ (ppm): 136.04 ($\nu_{1/2}$ = 360 Hz), 75.55 ($\nu_{1/2}$ = 480 Hz), 16.52 ($\nu_{1/2}$ = 960 Hz), 5.17 ($\nu_{1/2}$ = 360 Hz), and -148.95 ($\nu_{1/2}$ = 240 Hz). Elemental analysis calcd. (%) for $C_{36}H_{44}Cl_2F_{12}FeLi_2NO_6$ (955.35 g/mol): C 45.26, H 4.64, and N 1.47; found: C 45.17, H 4.65, and N 1.42.

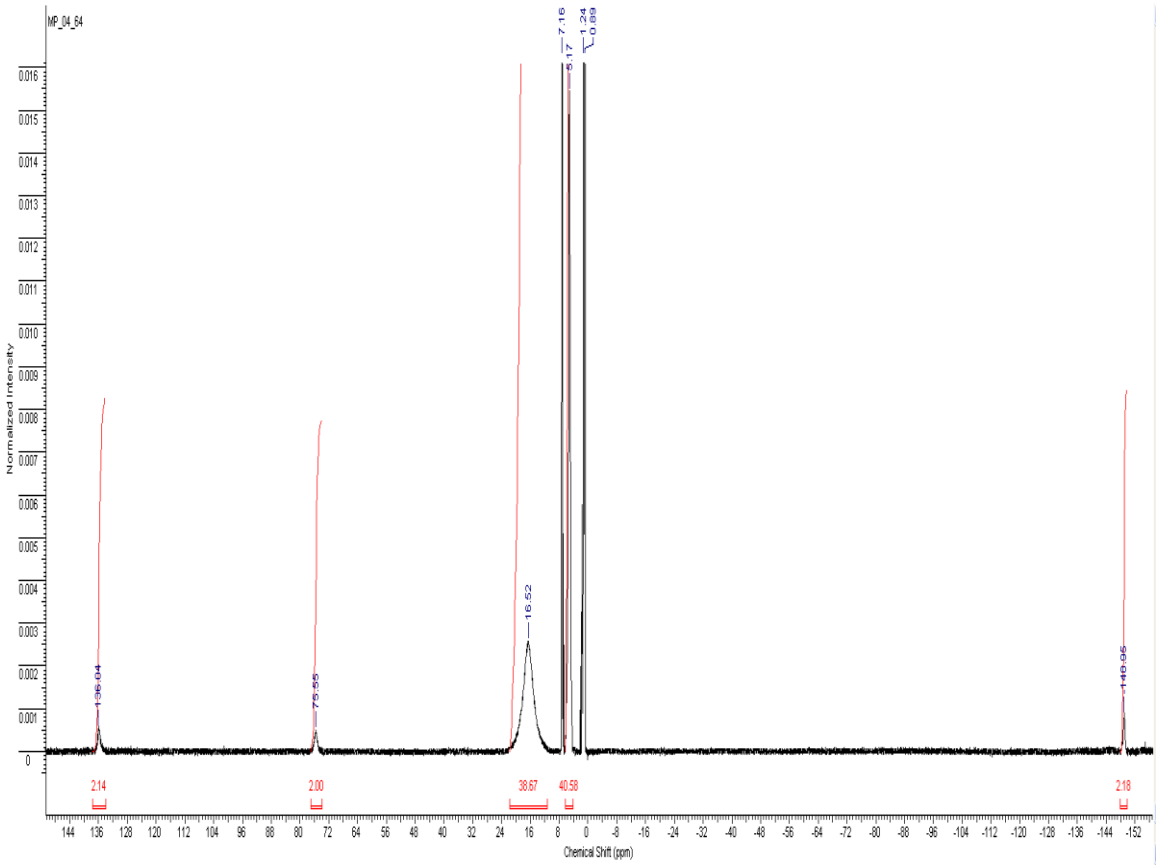

Figure S3. ^{1}H NMR spectrum of **3** in C_6D_6.

4. X-ray crystallography of 3

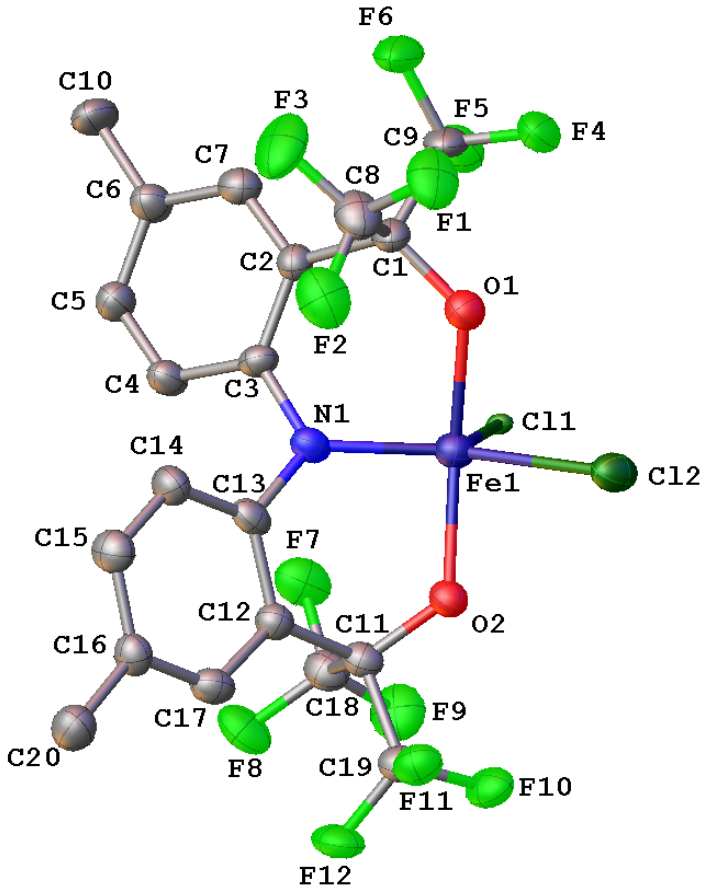

Figure S4. Molecular structure of **2**. Ellipsoids drawn at the 50 % probability level. Hydrogen atoms are omitted for clarity.

X-ray Experimental for 3.

X-Ray Intensity data were collected at 100 K on a Bruker **SMART** diffractometer using MoKα radiation (λ = 0.71073 Å) and an APEXII CCD area detector.

Raw data frames were read by program SAINT and integrated using 3D profiling algorithms. The resulting data were reduced to produce hkl reflections and their intensities and estimated standard deviations. The data were corrected for Lorentz and polarization effects and numerical absorption corrections were applied based on indexed and measured faces.

The structure was solved and refined in SHELXTL6.1, using full-matrix least-squares refinement. The non-H atoms were refined with anisotropic thermal parameters and all of the H atoms were calculated in idealized positions and refined riding on their parent atoms. The asymmetric unit consists of the Fe complex, one pentane solvent molecule in a general position and a half toluene solvent molecule (located on a 2-fold rotation symmetry). The solvent molecules were disordered and could not be modeled properly, thus program SQUEEZE, a part of the PLATON package of crystallographic software, was used to calculate the solvent disorder area and remove its contribution to the overall intensity data. In the final cycle of refinement, 11200 reflections (of which 4907 are observed with $I > 2\sigma(I)$) were used to refine 541 parameters and the resulting R_1, wR_2 and S (goodness of fit) were 6.79%, 17.50% and 0.856, respectively. The refinement was carried out by minimizing the wR_2 function using F^2 rather than F values. R_1 is calculated to provide a reference to the conventional R value but its function is not minimized.

Table S7. Crystal data and structure refinement for **3**.

Identification code	pasc3	
Empirical formula	$C_{36}H_{44}Cl_2F_{12}FeLi_2NO_6$	
Formula weight	955.35	
Temperature	100(2) K	
Wavelength	0.71073 Å	
Crystal system	Monoclinic	
Space group	C2/c	
Unit cell dimensions	a = 31.479(2) Å	α = 90°.
	b = 12.6762(10) Å	β = 117.561(4)°.
	c = 27.582(2) Å	γ = 90°.
Volume	9757.1(13) $Å^3$	
Z	8	
Density (calculated)	1.301 Mg/m^3	
Absorption coefficient	0.502 mm^{-1}	
F(000)	3912	
Crystal size	0.30 x 0.06 x 0.05 mm^3	
Theta range for data collection	1.63 to 27.50°.	
Index ranges	-40≤h≤40, -16≤k≤16, -35≤l≤35	
Reflections collected	77038	
Independent reflections	11200 [R(int) = 0.1505]	
Completeness to theta = 27.50°	100.0 %	
Absorption correction	Numerical	
Max. and min. transmission	0.9763 and 0.8639	
Refinement method	Full-matrix least-squares on F^2	
Data / restraints / parameters	11200 / 0 / 541	
Goodness-of-fit on F^2	0.856	
Final R indices [I>2sigma(I)]	R1 = 0.0679, wR2 = 0.1750 [4907]	
R indices (all data)	R1 = 0.1454, wR2 = 0.1975	
Largest diff. peak and hole	1.952 and -0.611 $e.Å^{-3}$	

$R1 = \Sigma(||F_o| - |F_c||) / \Sigma|F_o|$

$wR2 = [\Sigma[w(F_o^2 - F_c^2)^2] / \Sigma[w(F_o^2)^2]]^{1/2}$

$S = [\Sigma[w(F_o^2 - F_c^2)^2] / (n-p)]^{1/2}$

$w= 1/[\sigma^2(F_o^2)+(m*p)^2+n*p]$, $p = [\max(F_o^2,0)+ 2* F_c^2]/3$, m & n are constants.

Table S8. Atomic coordinates (x 10^4) and equivalent isotropic dispacement parameters ($Å^2$x 10^3) for **3**. U(eq) is defined as one third of the trace of the orthogonalized U^{ij} tensor.

Atom	x	y	z	U(eq)
Fe1	3469(1)	1483(1)	3844(1)	28(1)
Cl1	2962(1)	2499(1)	3108(1)	9(1)
Cl2	3976(1)	573(1)	3532(1)	41(1)
F1	4915(1)	2861(3)	5077(1)	57(1)
F2	4424(1)	2037(3)	5279(1)	55(1)
F3	4585(1)	3665(3)	5504(1)	68(1)
F4	4540(1)	3966(2)	4133(1)	49(1)
F5	3851(1)	4669(2)	3900(1)	49(1)
F6	4447(1)	5011(3)	4688(2)	60(1)
F7	2375(1)	1298(2)	3704(1)	45(1)
F8	2062(1)	-100(3)	3843(1)	47(1)
F9	2121(1)	68(3)	3098(1)	50(1)
F10	2683(1)	-1583(2)	3234(1)	40(1)
F11	3188(1)	-1998(2)	4059(1)	38(1)
F12	2432(1)	-1944(2)	3821(1)	44(1)
Li1	4405(3)	2228(7)	3822(4)	39(2)
Li2	3314(3)	-623(8)	3206(4)	47(3)
O1	4019(1)	2466(3)	4182(1)	34(1)
O2	3143(1)	104(3)	3705(1)	29(1)
O3	4356(1)	2804(3)	3147(1)	43(1)
O4	5051(1)	1680(3)	4171(2)	49(1)
O5	3642(1)	-1974(3)	3270(2)	45(1)
O6	2952(1)	-442(3)	2433(1)	47(1)
N1	3359(1)	1658(3)	4471(2)	29(1)
C1	4086(2)	3275(4)	4554(2)	31(1)
C2	3645(2)	3514(4)	4650(2)	28(1)
C3	3335(2)	2709(4)	4636(2)	27(1)
C4	2956(2)	2985(4)	4757(2)	33(1)
C5	2900(2)	3985(4)	4895(2)	37(1)
C6	3212(2)	4778(4)	4919(2)	36(1)
C7	3577(2)	4520(4)	4797(2)	36(1)
C8	4502(2)	2957(5)	5100(2)	46(2)
C9	4231(2)	4231(5)	4324(2)	44(2)
C10	3149(2)	5906(4)	5065(3)	53(2)
C11	2852(2)	-273(4)	3924(2)	29(1)
C12	3061(2)	-112(4)	4537(2)	27(1)
C13	3294(2)	852(4)	4779(2)	29(1)
C14	3493(2)	948(4)	5349(2)	33(1)
C15	3463(2)	170(4)	5677(2)	36(1)

C16	3230(2)	-779(4)	5450(2)	31(1)
C17	3033(2)	-881(4)	4888(2)	32(1)
C18	2354(2)	251(4)	3644(2)	35(1)
C19	2787(2)	-1454(4)	3762(2)	34(1)
C20	3207(2)	-1658(4)	5801(2)	45(2)
C21	3950(2)	3373(5)	2762(2)	48(2)
C22	3719(2)	2686(6)	2272(3)	70(2)
C23	4144(3)	2092(7)	2271(3)	98(3)
C24	4531(2)	2188(6)	2834(2)	65(2)
C25	5183(2)	836(5)	4563(3)	64(2)
C26	5704(2)	975(5)	4952(3)	54(2)
C27	5810(2)	2100(5)	4853(3)	60(2)
C28	5474(2)	2258(6)	4260(3)	65(2)
C29	4124(2)	-2250(6)	3597(3)	76(2)
C30	4237(2)	-3200(5)	3368(3)	61(2)
C31	3759(2)	-3566(5)	2915(3)	68(2)
C32	3407(2)	-2956(5)	3026(3)	62(2)
C33	2515(2)	131(5)	2151(2)	44(2)
C34	2454(3)	313(7)	1588(3)	77(2)
C35	2739(3)	-460(7)	1506(3)	83(2)
C36	3135(3)	-689(7)	2051(3)	87(3)

Table S9. Bond lengths (Å) for **3**.

Bond	Length (Å)	Bond	Length (Å)
Fe1-N1	1.926(4)	O6-C33	1.426(6)
Fe1-O2	1.973(3)	O6-C36	1.449(7)
Fe1-O1	1.980(3)	N1-C13	1.403(6)
Fe1-Cl1	2.3100(11)	N1-C3	1.421(6)
Fe1-Cl2	2.4252(15)	C1-C8	1.523(7)
Fe1-Li2	3.110(9)	C1-C9	1.531(7)
Fe1-Li1	3.122(8)	C1-C2	1.558(7)
Cl2-Li2	2.391(10)	C2-C7	1.384(7)
Cl2-Li1	2.423(9)	C2-C3	1.401(6)
F1-C8	1.338(6)	C3-C4	1.422(7)
F2-C8	1.333(7)	C4-C5	1.358(7)
F3-C8	1.357(7)	C5-C6	1.388(7)
F4-C9	1.348(6)	C6-C7	1.377(7)
F4-Li1	2.331(10)	C6-C10	1.524(7)
F5-C9	1.346(7)	C11-C12	1.519(7)
F6-C9	1.348(6)	C11-C18	1.542(7)
F7-C18	1.334(6)	C11-C19	1.549(7)
F8-C18	1.346(6)	C12-C17	1.405(7)
F9-C18	1.356(6)	C12-C13	1.422(7)
F10-C19	1.348(6)	C13-C14	1.402(7)
F10-Li2	2.362(11)	C14-C15	1.372(7)
F11-C19	1.335(6)	C15-C16	1.397(7)
F12-C19	1.351(6)	C16-C17	1.384(7)
Li1-O1	1.918(9)	C16-C20	1.499(7)
Li1-O4	1.930(9)	C21-C22	1.484(8)
Li1-O3	1.937(10)	C22-C23	1.535(9)
Li2-O6	1.911(11)	C23-C24	1.470(9)
Li2-O2	1.928(11)	C25-C26	1.497(8)
Li2-O5	1.965(10)	C26-C27	1.518(8)
O1-C1	1.396(6)	C27-C28	1.493(9)
O2-C11	1.395(6)	C29-C30	1.479(8)
O3-C21	1.425(6)	C30-C31	1.516(9)
O3-C24	1.450(7)	C31-C32	1.493(9)
O4-C28	1.439(7)	C33-C34	1.491(8)
O4-C25	1.439(7)	C34-C35	1.417(10)
O5-C29	1.405(6)	C35-C36	1.473(10)
O5-C32	1.445(6)		

Table S10. Bond angles (°) for **3**.

Bond	Angle (°)	Bond	Angle (°)
N1-Fe1-O2	89.04(15)	O1-C1-C8	107.5(4)
N1-Fe1-O1	89.19(15)	O1-C1-C9	104.5(4)
O2-Fe1-O1	155.72(14)	C8-C1-C9	109.6(4)
N1-Fe1-Cl1	112.74(12)	O1-C1-C2	115.0(4)
O2-Fe1-Cl1	103.69(10)	C8-C1-C2	108.1(4)
O1-Fe1-Cl1	99.31(10)	C9-C1-C2	112.0(4)
N1-Fe1-Cl2	142.53(12)	C7-C2-C3	118.6(5)
O2-Fe1-Cl2	82.96(10)	C7-C2-C1	120.0(4)
O1-Fe1-Cl2	83.8(1)	C3-C2-C1	121.2(4)
Cl1-Fe1-Cl2	104.71(5)	C2-C3-N1	123.5(4)
N1-Fe1-Li2	124.1(2)	C2-C3-C4	117.6(4)
O2-Fe1-Li2	36.6(2)	N1-C3-C4	118.7(4)
O1-Fe1-Li2	132.9(2)	C5-C4-C3	121.9(5)
Cl1-Fe1-Li2	96.70(18)	C4-C5-C6	120.5(5)
Cl2-Fe1-Li2	49.29(19)	C7-C6-C5	118.0(5)
N1-Fe1-Li1	123.1(2)	C7-C6-C10	120.9(5)
O2-Fe1-Li1	132.4(2)	C5-C6-C10	121.1(5)
O1-Fe1-Li1	36.1(2)	C6-C7-C2	123.4(5)
Cl1-Fe1-Li1	95.13(17)	F2-C8-F1	106.8(5)
Cl2-Fe1-Li1	49.87(18)	F2-C8-F3	105.9(5)
Li2-Fe1-Li1	98.7(3)	F1-C8-F3	106.0(4)
Li2-Cl2-Li1	158.4(3)	F2-C8-C1	112.1(4)
Li2-Cl2-Fe1	80.4(2)	F1-C8-C1	112.8(5)
Li1-Cl2-Fe1	80.2(2)	F3-C8-C1	112.8(5)
C9-F4-Li1	109.7(3)	F5-C9-F4	106.0(5)
C19-F10-Li2	100.7(4)	F5-C9-F6	106.5(5)
O1-Li1-O4	124.8(5)	F4-C9-F6	105.4(4)
O1-Li1-O3	130.6(5)	F5-C9-C1	111.8(4)
O4-Li1-O3	102.3(4)	F4-C9-C1	111.8(5)
O1-Li1-F4	73.3(3)	F6-C9-C1	114.6(5)
O4-Li1-F4	100.7(4)	O2-C11-C12	113.8(4)
O3-Li1-F4	85.3(4)	O2-C11-C18	110.8(4)
O1-Li1-Cl2	85.2(3)	C12-C11-C18	108.4(4)
O4-Li1-Cl2	98.7(4)	O2-C11-C19	103.5(4)
O3-Li1-Cl2	103.0(4)	C12-C11-C19	112.5(4)
F4-Li1-Cl2	156.7(4)	C18-C11-C19	107.7(4)
O1-Li1-Fe1	37.46(19)	C17-C12-C13	117.2(5)
O4-Li1-Fe1	131.8(4)	C17-C12-C11	122.8(4)
O3-Li1-Fe1	118.4(4)	C13-C12-C11	120.0(4)
F4-Li1-Fe1	107.0(3)	C14-C13-N1	120.0(4)

Cl2-Li1-Fe1	49.95(16)	C14-C13-C12	117.7(5)
O6-Li2-O2	121.4(5)	N1-C13-C12	122.1(5)
O6-Li2-O5	102.8(5)	C15-C14-C13	123.1(5)
O2-Li2-O5	131.4(6)	C14-C15-C16	120.3(5)
O6-Li2-F10	91.3(4)	C17-C16-C15	116.9(5)
O2-Li2-F10	73.0(4)	C17-C16-C20	121.6(5)
O5-Li2-F10	87.9(4)	C15-C16-C20	121.5(5)
O6-Li2-Cl2	108.1(5)	C16-C17-C12	124.7(5)
O2-Li2-Cl2	84.8(4)	F7-C18-F8	106.4(4)
O5-Li2-Cl2	100.9(4)	F7-C18-F9	106.3(4)
F10-Li2-Cl2	156.1(5)	F8-C18-F9	106.0(4)
O6-Li2-Fe1	112.7(4)	F7-C18-C11	112.6(4)
O2-Li2-Fe1	37.6(2)	F8-C18-C11	112.4(4)
O5-Li2-Fe1	139.4(4)	F9-C18-C11	112.6(4)
F10-Li2-Fe1	109.8(4)	F11-C19-F10	106.8(4)
Cl2-Li2-Fe1	50.27(18)	F11-C19-F12	106.7(4)
C1-O1-Li1	125.4(4)	F10-C19-F12	105.8(4)
C1-O1-Fe1	127.7(3)	F11-C19-C11	111.1(4)
Li1-O1-Fe1	106.4(3)	F10-C19-C11	111.2(4)
C11-O2-Li2	126.9(4)	F12-C19-C11	114.7(4)
C11-O2-Fe1	127.3(3)	O3-C21-C22	105.9(5)
Li2-O2-Fe1	105.7(3)	C21-C22-C23	103.3(5)
C21-O3-C24	106.6(4)	C24-C23-C22	104.8(6)
C21-O3-Li1	123.6(4)	O3-C24-C23	108.4(5)
C24-O3-Li1	119.1(5)	O4-C25-C26	106.9(5)
C28-O4-C25	109.0(4)	C25-C26-C27	104.0(5)
C28-O4-Li1	125.5(4)	C28-C27-C26	102.6(5)
C25-O4-Li1	121.0(4)	O4-C28-C27	104.5(5)
C29-O5-C32	104.6(4)	O5-C29-C30	109.2(5)
C29-O5-Li2	129.9(5)	C29-C30-C31	105.0(5)
C32-O5-Li2	125.1(4)	C32-C31-C30	102.7(5)
C33-O6-C36	108.8(4)	O5-C32-C31	105.9(5)
C33-O6-Li2	126.6(4)	O6-C33-C34	105.9(5)
C36-O6-Li2	123.5(5)	C35-C34-C33	105.9(6)
C13-N1-C3	116.4(4)	C34-C35-C36	105.8(6)
C13-N1-Fe1	126.6(3)	O6-C36-C35	105.4(6)
C3-N1-Fe1	117.0(3)		

Table S11. Anisotropic displacement parameters ($Å^2 x\ 10^3$) for **3**. The anisotropic displacement factor exponent takes the form: $-2\pi^2[\ h^2\ a^{*2}U^{11} + ...\ + 2\ h\ k\ a^*\ b^*\ U^{12}\ ]$.

Atom	U_{11}	U_{22}	U_{33}	U_{23}	U_{13}	U_{12}
Fe1	25(1)	26(1)	30(1)	1(1)	11(1)	-1(1)
Cl1	9(1)	7(1)	8(1)	2(1)	1(1)	1(1)
Cl2	36(1)	34(1)	60(1)	-8(1)	28(1)	-5(1)
F1	25(2)	91(3)	51(2)	-7(2)	14(2)	-2(2)
F2	40(2)	71(3)	50(2)	15(2)	17(2)	11(2)
F3	43(2)	105(3)	41(2)	-29(2)	8(2)	-5(2)
F4	54(2)	45(2)	66(2)	-12(2)	43(2)	-16(2)
F5	59(2)	42(2)	55(2)	8(2)	33(2)	-3(2)
F6	62(2)	53(2)	82(3)	-33(2)	48(2)	-32(2)
F7	32(2)	41(2)	56(2)	11(2)	15(2)	8(1)
F8	27(2)	57(2)	57(2)	12(2)	20(2)	-3(1)
F9	35(2)	67(2)	31(2)	5(2)	1(1)	5(2)
F10	44(2)	38(2)	28(2)	-5(1)	9(1)	-9(1)
F11	41(2)	29(2)	37(2)	1(1)	13(1)	1(1)
F12	42(2)	39(2)	48(2)	-5(2)	18(2)	-20(1)
Li1	28(5)	47(6)	48(6)	10(4)	24(4)	4(4)
Li2	44(6)	39(6)	49(6)	-7(5)	15(5)	5(4)
O1	32(2)	34(2)	37(2)	-1(2)	18(2)	-2(2)
O2	26(2)	31(2)	30(2)	0(2)	13(2)	-3(1)
O3	37(2)	54(3)	35(2)	1(2)	15(2)	4(2)
O4	30(2)	60(3)	50(2)	17(2)	13(2)	5(2)
O5	29(2)	38(2)	53(2)	-8(2)	6(2)	6(2)
O6	49(2)	58(3)	32(2)	-4(2)	19(2)	17(2)
N1	28(2)	24(2)	36(2)	2(2)	17(2)	-1(2)
C1	30(3)	33(3)	31(3)	-9(2)	15(2)	-11(2)
C2	27(3)	31(3)	29(3)	-5(2)	14(2)	-4(2)
C3	32(3)	20(3)	29(3)	-2(2)	13(2)	-3(2)
C4	35(3)	25(3)	44(3)	0(2)	24(3)	-3(2)
C5	44(3)	31(3)	45(3)	-4(3)	28(3)	-3(2)
C6	40(3)	27(3)	47(3)	0(3)	26(3)	-1(2)
C7	37(3)	32(3)	38(3)	-4(2)	18(3)	-8(2)
C8	31(3)	63(4)	40(3)	-4(3)	14(3)	-8(3)
C9	46(3)	38(3)	53(4)	-20(3)	29(3)	-24(3)
C10	69(4)	31(3)	77(5)	-20(3)	50(4)	-16(3)
C11	24(3)	29(3)	31(3)	1(2)	11(2)	-3(2)
C12	27(3)	26(3)	29(3)	1(2)	13(2)	0(2)
C13	25(3)	27(3)	39(3)	4(2)	19(2)	0(2)
C14	39(3)	34(3)	31(3)	1(2)	19(3)	-5(2)

C15	38(3)	38(3)	29(3)	3(2)	13(2)	-2(2)
C16	35(3)	32(3)	30(3)	5(2)	17(2)	3(2)
C17	32(3)	25(3)	41(3)	1(2)	17(3)	-2(2)
C18	29(3)	38(3)	34(3)	2(3)	11(2)	-3(2)
C19	29(3)	32(3)	36(3)	-1(3)	11(2)	-5(2)
C20	56(4)	39(3)	46(3)	-2(3)	29(3)	-2(3)
C21	41(3)	59(4)	45(4)	7(3)	22(3)	13(3)
C22	51(4)	84(5)	54(4)	-15(4)	5(3)	18(4)
C23	61(5)	139(8)	65(5)	-37(5)	5(4)	44(5)
C24	56(4)	104(6)	42(4)	2(4)	29(3)	29(4)
C25	49(4)	52(4)	71(5)	23(4)	12(4)	7(3)
C26	42(3)	52(4)	59(4)	11(3)	15(3)	7(3)
C27	37(3)	58(4)	77(5)	1(4)	20(3)	-3(3)
C28	29(3)	82(5)	74(5)	32(4)	16(3)	-1(3)
C29	39(4)	84(6)	71(5)	-24(4)	-3(3)	24(4)
C30	51(4)	44(4)	84(5)	7(4)	29(4)	9(3)
C31	79(5)	40(4)	67(5)	-17(4)	18(4)	13(4)
C32	39(3)	33(3)	90(5)	-21(4)	9(3)	-6(3)
C33	44(3)	39(3)	34(3)	1(3)	5(3)	6(3)
C34	56(4)	115(7)	56(5)	32(5)	24(4)	30(4)
C35	119(7)	95(6)	46(4)	7(4)	46(5)	7(5)
C36	89(6)	131(8)	50(5)	4(5)	39(4)	46(5)

5. Synthesis of 4.

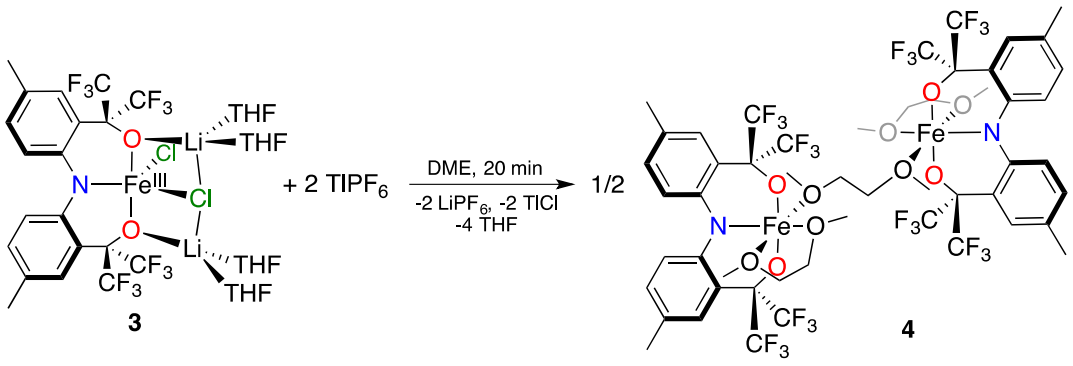

Figure S5. Synthesis of **4**.

Complex **3** (200 mg, 0.209 mmol) was dissolved in DME (1 mL) forming a blue solution. Two equivalents of $TlPF_6$, 97% (150 mg, 0.416 mmol) were also dissolved in DME (1 mL) and added dropwise to the former solution causing immediate precipitation of TlCl. The resulting green solution was stirred for 20 minutes, filtered through celite, and the solvent was removed under reduced pressure. After washing the green residue with pentane (5 mL), the resulting green powder was dissolved in 3 mL of a 2:1 pentane/DME mixture and filtered to remove the remaining inorganic salts. The solvent was removed under reduced pressure. Finally, the green powder was washed with pentane (5 mL) and dried under vacuum. Yield (0.056 g, 37.3 %). ^{1}H-NMR (C_6D_6, 300 MHz, 25 °C): δ (ppm) = 148.54 ($\nu_{1/2}$ = 360 Hz), 88.38 ($\nu_{1/2}$ = 360 Hz), 77.11 ($\nu_{1/2}$ = 2880 Hz), and -107.93 ($\nu_{1/2}$ = 600 Hz). Elemental analysis calcd (%) for $C_{52}H_{54}F_{24}Fe_2N_2O_{10}$ (1434.64 g/mol): C 43.53, H 3.79, and N 1.95; found: C 43.49, H 3.77, and N 2.00.

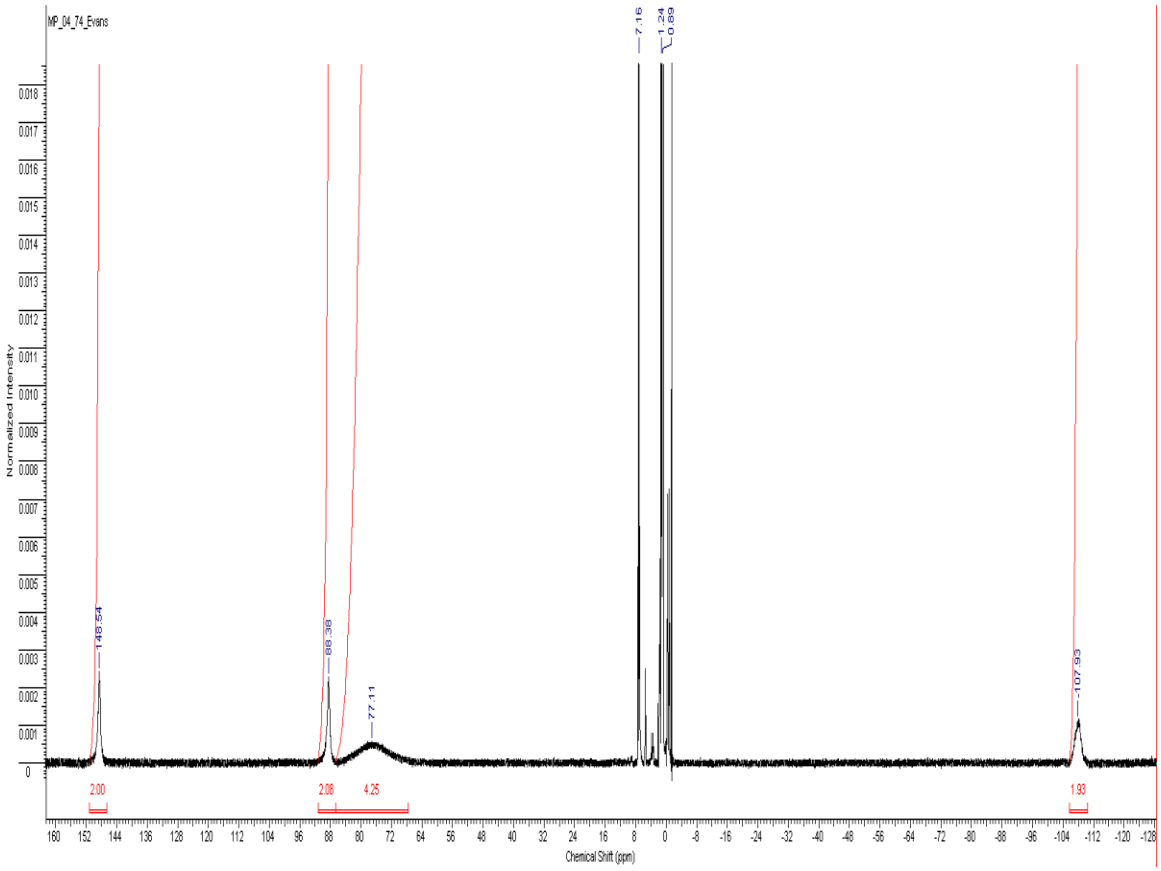

Figure S6. ^{1}H NMR spectrum of **4** in C_6D_6

6. X-ray crystallography of 4.

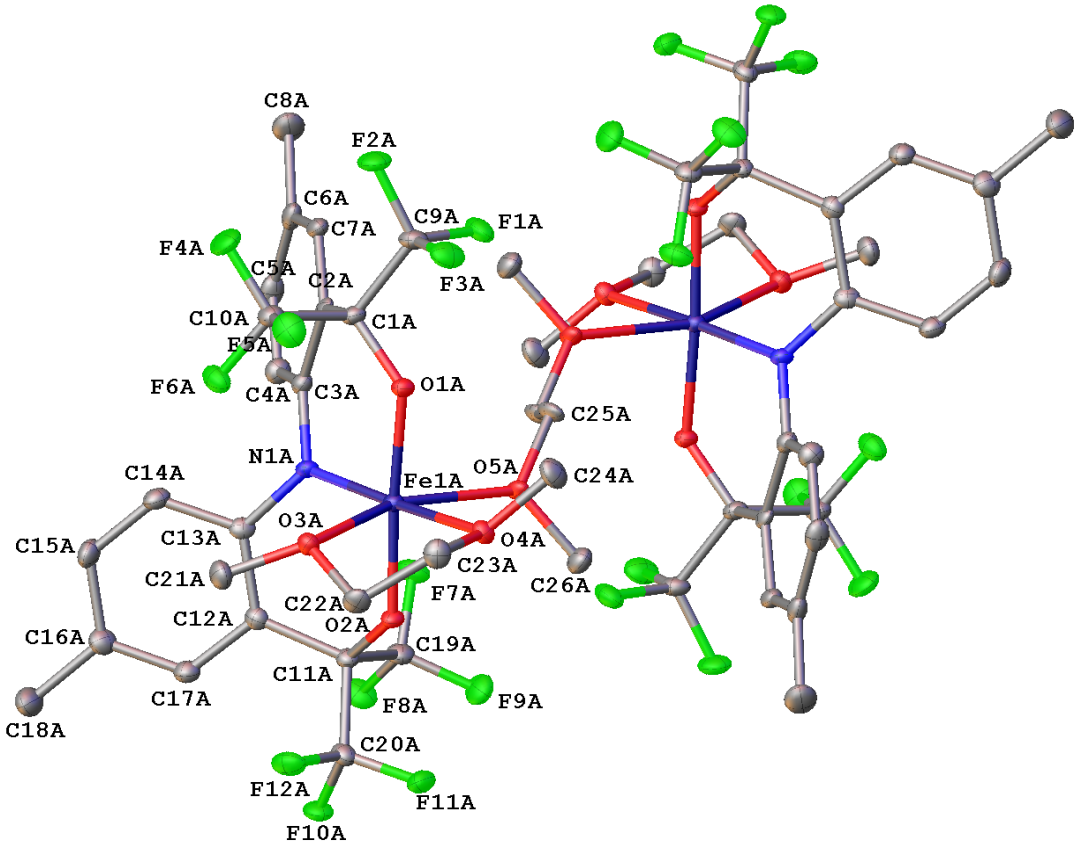

Figure S7. Molecular structure of **4**. Ellipsoids shown at the 50 % probability level. Hydrogen atoms are omitted for clarity

X-ray Experimental for 4.

X-Ray Intensity data were collected at 100 K on a Bruker **DUO** diffractometer using MoKα radiation (λ = 0.71073 Å) and an APEXII CCD area detector. Raw data frames were read by program SAINT and integrated using 3D profiling algorithms. The resulting data were reduced to produce hkl reflections and their intensities and estimated standard deviations. The data were corrected for Lorentz and polarization effects and numerical absorption corrections were applied based on indexed and measured faces.

The structure was solved and refined in SHELXTL6.1, using full-matrix least-squares refinement. The non-H atoms were refined with anisotropic thermal parameters and all of the H atoms were calculated in idealized positions and refined riding on their parent atoms. The asymmetric unit consists of two half-dimers (each located on an inversion center). The dimers comprise two Fe units with a DME molecule linking them together. Both dimers are chemically equivalent but crystallographically independent. In one dimer the $-CH_2CH_2-$ unit is disordered and was refined in two parts with their site occupation factors dependently refined. In the final cycle of refinement, 12245 reflections (of which 7194 are observed with $I > 2\sigma(I)$) were used to refine 820 parameters and the resulting R_1, wR_2 and S (goodness of fit) were 3.72%, 6.26% and 0.821, respectively. The refinement was carried out by minimizing the wR_2 function using F^2 rather than F values. R_1 is calculated to provide a reference to the conventional R value but its function is not minimized.

Table S12. Crystal data and structure refinement for **4**.

Identification code	pasc8	
Empirical formula	$C_{52}H_{54}F_{24}Fe_2N_2O_{10}$	
Formula weight	717.34	
Temperature	100(2) K	
Wavelength	0.71073 Å	
Crystal system	Triclinic	
Space group	P-1	
Unit cell dimensions	a = 12.2812(8) Å	α = 77.720(2)°.
	b = 13.3854(9) Å	β = 86.605(2)°.
	c = 18.4188(13) Å	γ = 77.097(2)°.
Volume	2883.6(3) $Å^3$	
Z	2	
Density (calculated)	1.652 Mg/m^3	
Absorption coefficient	0.639 mm^{-1}	
F(000)	1456	
Crystal size	0.10 x 0.05 x 0.03 mm^3	
Theta range for data collection	1.59 to 26.74°.	
Index ranges	-15≤h≤15, -16≤k≤16, -23≤l≤23	
Reflections collected	48530	
Independent reflections	12245 [R(int) = 0.0690]	
Completeness to theta = 26.74°	99.8 %	
Absorption correction	Numerical	
Max. and min. transmission	0.9842 and 0.9389	
Refinement method	Full-matrix least-squares on F^2	
Data / restraints / parameters	12245 / 0 / 820	
Goodness-of-fit on F^2	0.821	
Final R indices [I>2sigma(I)]	R1 = 0.0372, wR2 = 0.0626 [7194]	
R indices (all data)	R1 = 0.0858, wR2 = 0.0705	
Largest diff. peak and hole	0.451 and -0.533 $e.Å^{-3}$	

$R1 = \Sigma(||F_o| - |F_c||) / \Sigma|F_o|$

$wR2 = [\Sigma[w(F_o^2 - F_c^2)^2] / \Sigma[w(F_o^2)^2]]^{1/2}$

$S = [\Sigma[w(F_o^2 - F_c^2)^2] / (n-p)]^{1/2}$

$w= 1/[\sigma^2(F_o^2)+(m*p)^2+n*p]$, $p = [\max(F_o^2,0)+ 2* F_c^2]/3$, m & n are constants.

Table S13. Atomic coordinates (x 10^4) and equivalent isotropic displacement parameters ($Å^2$x 10^3) for **4**. U(eq) is defined as one third of the trace of the orthogonalized U^{ij} tensor.

Atom	x	y	z	U(eq)
Fe1A	8210(1)	7562(1)	9820(1)	11(1)
F1A	11876(1)	6967(1)	9537(1)	22(1)
F2A	12168(1)	8381(1)	8814(1)	24(1)
F3A	11448(1)	8434(1)	9895(1)	24(1)
F4A	10458(1)	9675(1)	8102(1)	27(1)
F5A	9762(1)	9955(1)	9161(1)	25(1)
F6A	8786(1)	9507(1)	8403(1)	22(1)
F7A	7443(1)	5418(1)	9364(1)	20(1)
F8A	5715(1)	5412(1)	9233(1)	23(1)
F9A	6388(1)	5153(1)	10328(1)	24(1)
F10A	4143(1)	6792(1)	9769(1)	21(1)
F11A	5035(1)	6810(1)	10728(1)	22(1)
F12A	4584(1)	8218(1)	9898(1)	23(1)
O1A	9630(1)	7899(1)	9666(1)	13(1)
O2A	6823(1)	7179(1)	10040(1)	13(1)
O3A	7312(1)	9207(1)	9767(1)	15(1)
O4A	8345(1)	7867(1)	10956(1)	14(1)
O5A	8976(1)	5984(1)	10393(1)	14(1)
N1A	8148(2)	7460(2)	8785(1)	12(1)
C1A	10230(2)	8155(2)	9027(1)	14(1)
C2A	10139(2)	7512(2)	8442(1)	13(1)
C3A	9124(2)	7219(2)	8347(1)	13(1)
C4A	9127(2)	6614(2)	7810(1)	17(1)
C5A	10040(2)	6338(2)	7366(1)	20(1)
C6A	11031(2)	6644(2)	7445(1)	18(1)
C7A	11049(2)	7222(2)	7983(1)	16(1)
C8A	12061(2)	6337(2)	6984(2)	27(1)
C9A	11441(2)	7989(2)	9314(2)	18(1)
C10A	9817(2)	9327(2)	8671(2)	18(1)
C11A	6108(2)	6912(2)	9602(1)	13(1)
C12A	6112(2)	7480(2)	8779(1)	14(1)
C13A	7109(2)	7703(2)	8422(1)	13(1)
C14A	7018(2)	8277(2)	7688(1)	17(1)
C15A	6023(2)	8595(2)	7314(2)	20(1)
C16A	5046(2)	8351(2)	7648(2)	19(1)
C17A	5121(2)	7793(2)	8377(1)	17(1)
C18A	3954(2)	8683(2)	7239(2)	30(1)
C19A	6408(2)	5720(2)	9638(2)	18(1)

C20A	4958(2)	7170(2)	9997(2)	17(1)
C21A	6500(2)	9763(2)	9209(2)	20(1)
C22A	6899(2)	9320(2)	10500(1)	18(1)
C23A	7873(2)	8935(2)	11000(2)	19(1)
C24A	9402(2)	7520(2)	11331(2)	22(1)
C25A	10058(2)	5394(2)	10226(2)	17(1)
C26A	8453(2)	5448(2)	11037(2)	21(1)
Fe1B	3398(1)	6490(1)	3403(1)	16(1)
F1B	-875(1)	6962(1)	4285(1)	33(1)
F2B	94(1)	5756(1)	3766(1)	38(1)
F3B	-253(1)	7356(1)	3168(1)	40(1)
F4B	498(1)	6914(1)	5371(1)	33(1)
F5B	1135(1)	5402(1)	5101(1)	36(1)
F6B	2258(1)	6393(1)	5179(1)	32(1)
F7B	6780(1)	6332(1)	2402(1)	28(1)
F8B	7390(1)	7490(1)	2806(1)	26(1)
F9B	7066(1)	6123(1)	3572(1)	25(1)
F10B	5708(1)	9045(1)	2374(1)	28(1)
F11B	5217(1)	8013(1)	1766(1)	33(1)
F12B	4035(1)	8804(1)	2474(1)	25(1)
O1B	1936(2)	6338(1)	3713(1)	22(1)
O2B	4858(1)	6615(1)	3065(1)	16(1)
O3B	2695(2)	7192(1)	2281(1)	23(1)
O4B	3601(2)	5176(2)	2798(1)	29(1)
O5B	4056(2)	5136(1)	4254(1)	29(1)
N1B	3237(2)	7699(2)	3863(1)	14(1)
C1B	1125(2)	6898(2)	4111(2)	17(1)
C2B	1167(2)	8063(2)	4012(1)	17(1)
C3B	2192(2)	8387(2)	3914(1)	16(1)
C4B	2139(2)	9471(2)	3799(2)	20(1)
C5B	1160(2)	10195(2)	3816(2)	24(1)
C6B	143(2)	9885(2)	3945(2)	23(1)
C7B	178(2)	8824(2)	4038(2)	22(1)
C8B	-938(2)	10665(2)	3972(2)	35(1)
C9B	19(3)	6740(3)	3839(2)	28(1)
C10B	1249(2)	6393(2)	4945(2)	23(1)
C11B	5437(2)	7378(2)	3079(1)	15(1)
C12B	5243(2)	7806(2)	3802(1)	14(1)
C13B	4171(2)	7949(2)	4144(1)	15(1)
C14B	4056(2)	8302(2)	4816(2)	18(1)
C15B	4934(2)	8555(2)	5120(2)	21(1)
C16B	5982(2)	8453(2)	4780(2)	20(1)
C17B	6104(2)	8079(2)	4128(2)	18(1)

C18B	6948(2)	8705(2)	5120(2)	28(1)
C19B	6676(2)	6843(2)	2961(2)	21(1)
C20B	5103(2)	8309(2)	2420(2)	20(1)
C21B	1921(2)	8176(2)	2105(2)	32(1)
C22B	2751(9)	6429(6)	1809(5)	26(2)
C23B	2679(9)	5427(6)	2277(5)	36(3)
C22C	2253(6)	6442(4)	2005(3)	23(2)
C23C	3236(6)	5535(4)	2022(3)	28(2)
C24B	4672(3)	4548(3)	2694(2)	56(1)
C25B	3454(3)	4280(2)	4454(2)	40(1)
C26B	5091(3)	4901(3)	4595(2)	37(1)

Table S14. Bond lengths (Å) for **4**.

Bond	Length (Å)	Bond	Length (Å)
Fe1A-O2A	1.8837(16)	Fe1B-N1B	1.949(2)
Fe1A-O1A	1.8878(17)	Fe1B-O5B	2.1645(19)
Fe1A-N1A	1.947(2)	Fe1B-O3B	2.2186(18)
Fe1A-O5A	2.1770(17)	Fe1B-O4B	2.2363(19)
Fe1A-O3A	2.2166(17)	F1B-C9B	1.349(3)
Fe1A-O4A	2.2383(17)	F2B-C9B	1.335(3)
F1A-C9A	1.336(3)	F3B-C9B	1.345(3)
F2A-C9A	1.351(3)	F4B-C10B	1.346(3)
F3A-C9A	1.333(3)	F5B-C10B	1.334(3)
F4A-C10A	1.339(3)	F6B-C10B	1.337(3)
F5A-C10A	1.348(3)	F7B-C19B	1.338(3)
F6A-C10A	1.338(3)	F8B-C19B	1.344(3)
F7A-C19A	1.347(3)	F9B-C19B	1.349(3)
F8A-C19A	1.348(3)	F10B-C20B	1.347(3)
F9A-C19A	1.336(3)	F11B-C20B	1.337(3)
F10A-C20A	1.342(3)	F12B-C20B	1.340(3)
F11A-C20A	1.331(3)	O1B-C1B	1.380(3)
F12A-C20A	1.351(3)	O2B-C11B	1.374(3)
O1A-C1A	1.372(3)	O3B-C21B	1.427(3)
O2A-C11A	1.377(3)	O3B-C22C	1.434(5)
O3A-C21A	1.438(3)	O3B-C22B	1.464(7)
O3A-C22A	1.439(3)	O4B-C24B	1.421(4)
O4A-C23A	1.435(3)	O4B-C23B	1.462(8)
O4A-C24A	1.442(3)	O4B-C23C	1.470(6)
O5A-C25A	1.439(3)	O5B-C26B	1.394(3)
O5A-C26A	1.445(3)	O5B-C25B	1.470(3)
N1A-C13A	1.416(3)	N1B-C3B	1.414(3)
N1A-C3A	1.420(3)	N1B-C13B	1.418(3)
C1A-C2A	1.540(3)	C1B-C2B	1.543(4)
C1A-C10A	1.548(4)	C1B-C10B	1.543(4)
C1A-C9A	1.561(4)	C1B-C9B	1.547(4)
C2A-C7A	1.396(3)	C2B-C7B	1.406(4)
C2A-C3A	1.417(3)	C2B-C3B	1.412(3)
C3A-C4A	1.404(3)	C3B-C4B	1.407(4)
C4A-C5A	1.377(3)	C4B-C5B	1.369(4)
C5A-C6A	1.392(4)	C5B-C6B	1.394(4)
C6A-C7A	1.384(4)	C6B-C7B	1.385(4)
C6A-C8A	1.511(4)	C6B-C8B	1.500(4)
C11A-C19A	1.544(4)	C11B-C20B	1.543(4)
C11A-C12A	1.545(3)	C11B-C12B	1.545(3)

C11A-C20A	1.552(4)	C11B-C19B	1.554(4)
C12A-C17A	1.397(3)	C12B-C17B	1.397(3)
C12A-C13A	1.416(3)	C12B-C13B	1.416(3)
C13A-C14A	1.404(3)	C13B-C14B	1.406(3)
C14A-C15A	1.376(4)	C14B-C15B	1.380(4)
C15A-C16A	1.388(4)	C15B-C16B	1.391(4)
C16A-C17A	1.388(4)	C16B-C17B	1.384(4)
C16A-C18A	1.508(4)	C16B-C18B	1.506(4)
C22A-C23A	1.483(4)	C22B-C23B	1.450(14)
C25A-C25A#1	1.511(5)	C22C-C23C	1.506(10)
Fe1B-O1B	1.8921(18)	C26B-C26B#2	1.564(6)
Fe1B-O2B	1.8949(17)		

Table S15. Bond angles (°) for **4**.

Bond	Angle (°)	Bond	Angle (°)
O2A-Fe1A-O1A	176.05(8)	O2B-Fe1B-O5B	91.29(8)
O2A-Fe1A-N1A	92.01(8)	N1B-Fe1B-O5B	105.89(8)
O1A-Fe1A-N1A	91.35(8)	O1B-Fe1B-O3B	86.85(8)
O2A-Fe1A-O5A	86.86(7)	O2B-Fe1B-O3B	92.00(7)
O1A-Fe1A-O5A	90.28(7)	N1B-Fe1B-O3B	103.01(8)
N1A-Fe1A-O5A	104.69(8)	O5B-Fe1B-O3B	150.85(7)
O2A-Fe1A-O3A	87.46(7)	O1B-Fe1B-O4B	91.01(7)
O1A-Fe1A-O3A	93.96(7)	O2B-Fe1B-O4B	87.10(7)
N1A-Fe1A-O3A	100.69(8)	N1B-Fe1B-O4B	175.96(8)
O5A-Fe1A-O3A	154.16(6)	O5B-Fe1B-O4B	77.65(7)
O2A-Fe1A-O4A	92.91(7)	O3B-Fe1B-O4B	73.61(7)
O1A-Fe1A-O4A	83.93(7)	C1B-O1B-Fe1B	132.05(16)
N1A-Fe1A-O4A	172.91(7)	C11B-O2B-Fe1B	131.06(15)
O5A-Fe1A-O4A	80.69(6)	C21B-O3B-C22C	107.7(3)
O3A-Fe1A-O4A	74.45(6)	C21B-O3B-C22B	119.1(4)
C1A-O1A-Fe1A	131.35(15)	C22C-O3B-C22B	27.5(3)
C11A-O2A-Fe1A	131.09(15)	C21B-O3B-Fe1B	123.85(17)
C21A-O3A-C22A	111.40(19)	C22C-O3B-Fe1B	109.9(2)
C21A-O3A-Fe1A	123.08(15)	C22B-O3B-Fe1B	113.6(3)
C22A-O3A-Fe1A	108.63(14)	C24B-O4B-C23B	124.6(4)
C23A-O4A-C24A	109.82(18)	C24B-O4B-C23C	100.1(3)
C23A-O4A-Fe1A	112.53(14)	C23B-O4B-C23C	32.8(3)
C24A-O4A-Fe1A	119.55(15)	C24B-O4B-Fe1B	121.00(19)
C25A-O5A-C26A	112.53(19)	C23B-O4B-Fe1B	107.8(3)
C25A-O5A-Fe1A	125.68(14)	C23C-O4B-Fe1B	112.6(2)
C26A-O5A-Fe1A	121.63(14)	C26B-O5B-C25B	113.0(2)
C13A-N1A-C3A	117.0(2)	C26B-O5B-Fe1B	126.92(18)
C13A-N1A-Fe1A	120.39(16)	C25B-O5B-Fe1B	119.65(17)
C3A-N1A-Fe1A	122.43(16)	C3B-N1B-C13B	116.6(2)
O1A-C1A-C2A	113.4(2)	C3B-N1B-Fe1B	121.84(17)
O1A-C1A-C10A	109.8(2)	C13B-N1B-Fe1B	121.51(17)
C2A-C1A-C10A	107.9(2)	O1B-C1B-C2B	114.2(2)
O1A-C1A-C9A	103.2(2)	O1B-C1B-C10B	109.1(2)
C2A-C1A-C9A	113.8(2)	C2B-C1B-C10B	108.1(2)
C10A-C1A-C9A	108.6(2)	O1B-C1B-C9B	103.7(2)
C7A-C2A-C3A	118.6(2)	C2B-C1B-C9B	112.9(2)
C7A-C2A-C1A	120.6(2)	C10B-C1B-C9B	108.6(2)
C3A-C2A-C1A	120.8(2)	C7B-C2B-C3B	118.4(2)
C4A-C3A-C2A	116.8(2)	C7B-C2B-C1B	120.4(2)
C4A-C3A-N1A	119.5(2)	C3B-C2B-C1B	121.2(2)

C2A-C3A-N1A	123.6(2)	C4B-C3B-C2B	116.9(2)
C5A-C4A-C3A	123.3(2)	C4B-C3B-N1B	119.3(2)
C4A-C5A-C6A	120.2(2)	C2B-C3B-N1B	123.6(2)
C7A-C6A-C5A	117.2(2)	C5B-C4B-C3B	123.2(3)
C7A-C6A-C8A	120.7(2)	C4B-C5B-C6B	120.8(3)
C5A-C6A-C8A	122.0(2)	C7B-C6B-C5B	116.7(3)
C6A-C7A-C2A	123.9(2)	C7B-C6B-C8B	121.7(3)
F3A-C9A-F1A	107.2(2)	C5B-C6B-C8B	121.6(3)
F3A-C9A-F2A	105.6(2)	C6B-C7B-C2B	123.9(3)
F1A-C9A-F2A	106.9(2)	F2B-C9B-F3B	106.7(2)
F3A-C9A-C1A	111.2(2)	F2B-C9B-F1B	106.1(2)
F1A-C9A-C1A	110.0(2)	F3B-C9B-F1B	105.9(2)
F2A-C9A-C1A	115.4(2)	F2B-C9B-C1B	111.9(2)
F6A-C10A-F4A	106.3(2)	F3B-C9B-C1B	110.9(2)
F6A-C10A-F5A	106.4(2)	F1B-C9B-C1B	114.8(2)
F4A-C10A-F5A	106.7(2)	F5B-C10B-F6B	107.0(2)
F6A-C10A-C1A	110.9(2)	F5B-C10B-F4B	106.9(2)
F4A-C10A-C1A	113.6(2)	F6B-C10B-F4B	106.6(2)
F5A-C10A-C1A	112.6(2)	F5B-C10B-C1B	113.1(2)
O2A-C11A-C19A	109.9(2)	F6B-C10B-C1B	110.4(2)
O2A-C11A-C12A	113.9(2)	F4B-C10B-C1B	112.5(2)
C19A-C11A-C12A	108.5(2)	O2B-C11B-C20B	110.6(2)
O2A-C11A-C20A	103.3(2)	O2B-C11B-C12B	113.1(2)
C19A-C11A-C20A	107.6(2)	C20B-C11B-C12B	107.9(2)
C12A-C11A-C20A	113.4(2)	O2B-C11B-C19B	104.1(2)
C17A-C12A-C13A	118.9(2)	C20B-C11B-C19B	108.0(2)
C17A-C12A-C11A	120.1(2)	C12B-C11B-C19B	113.0(2)
C13A-C12A-C11A	120.9(2)	C17B-C12B-C13B	118.4(2)
C14A-C13A-C12A	116.9(2)	C17B-C12B-C11B	121.3(2)
C14A-C13A-N1A	119.3(2)	C13B-C12B-C11B	120.3(2)
C12A-C13A-N1A	123.6(2)	C14B-C13B-C12B	117.6(2)
C15A-C14A-C13A	122.6(2)	C14B-C13B-N1B	119.0(2)
C14A-C15A-C16A	121.2(3)	C12B-C13B-N1B	123.3(2)
C15A-C16A-C17A	116.8(2)	C15B-C14B-C13B	121.9(3)
C15A-C16A-C18A	121.5(2)	C14B-C15B-C16B	121.3(3)
C17A-C16A-C18A	121.6(2)	C17B-C16B-C15B	116.9(2)
C16A-C17A-C12A	123.5(2)	C17B-C16B-C18B	121.7(2)
F9A-C19A-F7A	106.5(2)	C15B-C16B-C18B	121.4(2)
F9A-C19A-F8A	106.9(2)	C16B-C17B-C12B	123.9(3)
F7A-C19A-F8A	106.0(2)	F7B-C19B-F8B	106.1(2)
F9A-C19A-C11A	113.3(2)	F7B-C19B-F9B	106.5(2)
F7A-C19A-C11A	111.3(2)	F8B-C19B-F9B	106.5(2)
F8A-C19A-C11A	112.4(2)	F7B-C19B-C11B	111.1(2)

F11A-C20A-F10A	106.3(2)	F8B-C19B-C11B	115.4(2)
F11A-C20A-F12A	106.2(2)	F9B-C19B-C11B	110.7(2)
F10A-C20A-F12A	106.6(2)	F11B-C20B-F12B	106.6(2)
F11A-C20A-C11A	111.4(2)	F11B-C20B-F10B	106.8(2)
F10A-C20A-C11A	115.6(2)	F12B-C20B-F10B	105.8(2)
F12A-C20A-C11A	110.2(2)	F11B-C20B-C11B	112.5(2)
O3A-C22A-C23A	106.6(2)	F12B-C20B-C11B	111.7(2)
O4A-C23A-C22A	108.1(2)	F10B-C20B-C11B	113.0(2)
O5A-C25A-C25A#1	110.4(3)	C23B-C22B-O3B	108.8(7)
O1B-Fe1B-O2B	178.00(8)	C22B-C23B-O4B	105.4(8)
O1B-Fe1B-N1B	91.02(8)	O3B-C22C-C23C	103.7(5)
O2B-Fe1B-N1B	90.83(8)	O4B-C23C-C22C	107.1(5)
O1B-Fe1B-O5B	88.93(8)	O5B-C26B-C26B#2	108.7(3)

Symmetry transformations used to generate equivalent atoms:

#1 -x+2,-y+1,-z+2 #2 -x+1,-y+1,-z+1

Table S16. Anisotropic displacement parameters ($Å^2 x\ 10^3$) for **4**. The anisotropic displacement factor exponent takes the form: $-2\pi^2[h^2\ a^{*2}U^{11} + ...\ + 2\ h\ k\ a^*\ b^*\ U^{12}\ ]$.

Atom	U_{11}	U_{22}	U_{33}	U_{23}	U_{13}	U_{12}
Fe1A	10(1)	11(1)	13(1)	-2(1)	1(1)	-3(1)
F1A	12(1)	20(1)	32(1)	-1(1)	-4(1)	-2(1)
F2A	15(1)	28(1)	30(1)	-4(1)	6(1)	-11(1)
F3A	18(1)	34(1)	26(1)	-12(1)	-2(1)	-10(1)
F4A	26(1)	22(1)	29(1)	6(1)	8(1)	-10(1)
F5A	31(1)	15(1)	33(1)	-9(1)	-3(1)	-5(1)
F6A	16(1)	15(1)	31(1)	-1(1)	-4(1)	-3(1)
F7A	13(1)	17(1)	32(1)	-10(1)	2(1)	-3(1)
F8A	20(1)	20(1)	34(1)	-10(1)	-5(1)	-8(1)
F9A	28(1)	16(1)	27(1)	3(1)	0(1)	-8(1)
F10A	12(1)	24(1)	27(1)	-3(1)	1(1)	-8(1)
F11A	17(1)	30(1)	17(1)	-2(1)	3(1)	-8(1)
F12A	17(1)	18(1)	32(1)	-8(1)	7(1)	-1(1)
O1A	10(1)	16(1)	14(1)	-3(1)	1(1)	-4(1)
O2A	10(1)	16(1)	13(1)	-2(1)	0(1)	-6(1)
O3A	13(1)	14(1)	15(1)	-2(1)	0(1)	0(1)
O4A	13(1)	15(1)	15(1)	-4(1)	-2(1)	-1(1)
O5A	11(1)	11(1)	17(1)	0(1)	4(1)	2(1)
N1A	9(1)	14(1)	13(1)	-3(1)	3(1)	-3(1)
C1A	12(1)	15(2)	15(1)	-3(1)	3(1)	-5(1)
C2A	15(2)	9(1)	12(1)	3(1)	2(1)	-2(1)
C3A	14(2)	12(2)	12(1)	-1(1)	1(1)	-2(1)
C4A	18(2)	18(2)	16(2)	-4(1)	0(1)	-5(1)
C5A	28(2)	16(2)	12(2)	-5(1)	0(1)	1(1)
C6A	21(2)	16(2)	13(1)	2(1)	1(1)	2(1)
C7A	12(2)	17(2)	16(2)	3(1)	2(1)	-3(1)
C8A	24(2)	32(2)	21(2)	-8(1)	7(1)	1(1)
C9A	12(2)	20(2)	23(2)	-5(1)	4(1)	-6(1)
C10A	14(2)	19(2)	20(2)	-1(1)	2(1)	-6(1)
C11A	11(1)	13(2)	16(1)	-2(1)	0(1)	-5(1)
C12A	14(2)	11(1)	16(1)	-4(1)	0(1)	-2(1)
C13A	14(2)	14(2)	16(1)	-6(1)	1(1)	-6(1)
C14A	16(2)	20(2)	16(2)	-4(1)	3(1)	-8(1)
C15A	24(2)	23(2)	12(2)	1(1)	-2(1)	-8(1)
C16A	18(2)	23(2)	18(2)	-6(1)	-2(1)	-7(1)
C17A	14(2)	18(2)	19(2)	-3(1)	1(1)	-6(1)
C18A	22(2)	43(2)	22(2)	2(2)	-5(1)	-10(2)
C19A	13(2)	20(2)	21(2)	-4(1)	0(1)	-7(1)
C20A	12(2)	16(2)	22(2)	-2(1)	-2(1)	-4(1)

C21A	20(2)	16(2)	20(2)	0(1)	-3(1)	1(1)
C22A	17(2)	16(2)	19(2)	-7(1)	5(1)	2(1)
C23A	23(2)	16(2)	18(2)	-7(1)	0(1)	-3(1)
C24A	19(2)	28(2)	19(2)	-8(1)	-7(1)	-2(1)
C25A	8(1)	12(2)	26(2)	-2(1)	2(1)	3(1)
C26A	22(2)	18(2)	19(2)	3(1)	3(1)	-4(1)
Fe1B	18(1)	16(1)	16(1)	-3(1)	1(1)	-5(1)
F1B	17(1)	40(1)	42(1)	-6(1)	4(1)	-12(1)
F2B	36(1)	42(1)	46(1)	-19(1)	8(1)	-26(1)
F3B	38(1)	59(1)	28(1)	1(1)	-12(1)	-26(1)
F4B	35(1)	41(1)	19(1)	-4(1)	12(1)	-7(1)
F5B	44(1)	26(1)	34(1)	6(1)	6(1)	-14(1)
F6B	28(1)	45(1)	21(1)	6(1)	-6(1)	-12(1)
F7B	24(1)	35(1)	27(1)	-19(1)	4(1)	-3(1)
F8B	16(1)	34(1)	28(1)	-6(1)	6(1)	-10(1)
F9B	20(1)	25(1)	25(1)	-3(1)	-1(1)	3(1)
F10B	26(1)	22(1)	33(1)	2(1)	3(1)	-11(1)
F11B	52(1)	31(1)	13(1)	-3(1)	0(1)	-5(1)
F12B	20(1)	25(1)	26(1)	4(1)	-2(1)	-2(1)
O1B	20(1)	23(1)	26(1)	-11(1)	8(1)	-10(1)
O2B	16(1)	16(1)	18(1)	-5(1)	1(1)	-6(1)
O3B	27(1)	22(1)	20(1)	-6(1)	-5(1)	-5(1)
O4B	30(1)	22(1)	35(1)	-11(1)	-6(1)	1(1)
O5B	40(1)	19(1)	25(1)	2(1)	-5(1)	-5(1)
N1B	10(1)	16(1)	15(1)	-3(1)	1(1)	-3(1)
C1B	16(2)	18(2)	17(2)	-1(1)	4(1)	-8(1)
C2B	18(2)	20(2)	12(1)	-1(1)	-1(1)	-6(1)
C3B	16(2)	19(2)	12(1)	-2(1)	-1(1)	-3(1)
C4B	17(2)	20(2)	22(2)	-4(1)	6(1)	-6(1)
C5B	23(2)	18(2)	27(2)	1(1)	3(1)	-2(1)
C6B	17(2)	23(2)	25(2)	0(1)	0(1)	0(1)
C7B	13(2)	28(2)	23(2)	-1(1)	0(1)	-5(1)
C8B	22(2)	27(2)	46(2)	3(2)	4(2)	2(1)
C9B	28(2)	35(2)	23(2)	-1(2)	2(1)	-14(2)
C10B	20(2)	26(2)	23(2)	-2(1)	4(1)	-9(1)
C11B	13(2)	17(2)	14(1)	-3(1)	1(1)	-3(1)
C12B	12(2)	12(2)	16(1)	-1(1)	0(1)	-2(1)
C13B	15(2)	10(1)	17(2)	1(1)	-1(1)	-2(1)
C14B	17(2)	21(2)	18(2)	-8(1)	4(1)	-2(1)
C15B	24(2)	22(2)	19(2)	-11(1)	-1(1)	-3(1)
C16B	18(2)	20(2)	23(2)	-7(1)	-1(1)	-5(1)
C17B	13(2)	18(2)	24(2)	-4(1)	4(1)	-4(1)
C18B	19(2)	36(2)	35(2)	-18(2)	-3(1)	-7(1)

C19B	20(2)	25(2)	18(2)	-6(1)	2(1)	-6(1)
C20B	20(2)	22(2)	16(2)	-4(1)	4(1)	-6(1)
C21B	28(2)	32(2)	30(2)	6(2)	-10(1)	-3(2)
C24B	52(3)	43(2)	78(3)	-34(2)	8(2)	-1(2)
C25B	50(2)	25(2)	43(2)	4(2)	2(2)	-14(2)
C26B	38(2)	32(2)	40(2)	-5(2)	-9(2)	-7(2)

7. Synthesis of 5.

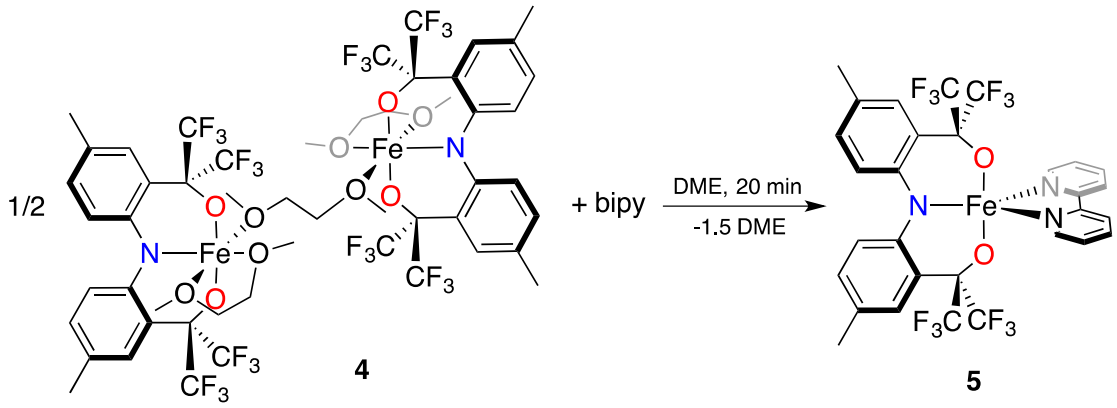

Figure S8. Synthesis of **5**, method a.

Method a) Complex **4** (80 mg, 0.056 mmol) was dissolved in DME (1 mL) and a DME (1 mL) solution of recrystallized 2,2'-bipyridine (18 mg, 0.115 mmol) was added dropwise producing a bluish green solution. After 20 minutes of stirring, the solvent was removed under reduced pressure and the solid was washed with pentane (5 mL). Another portion of pentane (2 mL) and DME (1 mL) was added, the resulting suspension was filtered through celite, and then the filtrate was concentrated under reduced pressure. Cooling a saturated DME/pentane solution to -35 °C yielded green crystals. Yield (0.041 g, 49.8 %). ^{1}H-NMR (C_6D_6, 300 MHz, 25 °C): δ = 118.72 ($\nu_{1/2}$ = 240 Hz), 92.28 ($\nu_{1/2}$ = 600 Hz), 74.09 ($\nu_{1/2}$ = 360 Hz), 68.13 (480 Hz), -10.79 ($\nu_{1/2}$ = 240 Hz), and -158.39 ($\nu_{1/2}$ = 960 Hz). Elemental analysis calcd (%) for $C_{30}H_{20}F_{12}FeN_3O_2$ (738.07 g/mol): C 48.80, H 2.73, and N 5.69; found: C 48.72, H 2.81, and N 5.76.

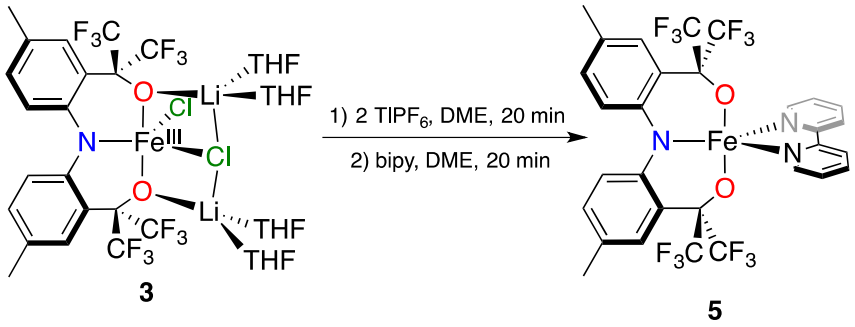

Figure S9. Synthesis of **5**, method b.

Method b) Complex **3** (200 mg, 0.209 mmol) was dissolved in DME (1 mL) forming a blue solution. $TlPF_6$, 97% (150 mg, 0.208 mmol) was also dissolved in DME (1 mL) and added dropwise to the former solution causing the immediate precipitation of TlCl. The resulting green solution was stirred for 20 minutes and then filtered through celite. A solution of recrystallized 2,2'-bipyridine (0.033 g, 0.211 mmol) in DME (1 mL) was added dropwise producing a bluish green solution. After 20 minutes of stirring, the solvent was removed under reduced pressure and the solid was washed with pentane (5 mL). Another portion of pentane (2 mL) and DME (1 mL) was added, the resulting suspension was filtered through celite, and then the filtrate was concentrated under reduced pressure. Cooling a saturated DME/pentane solution to -35 °C yielded green crystals. Yield (0.111 g, 71.8 %).

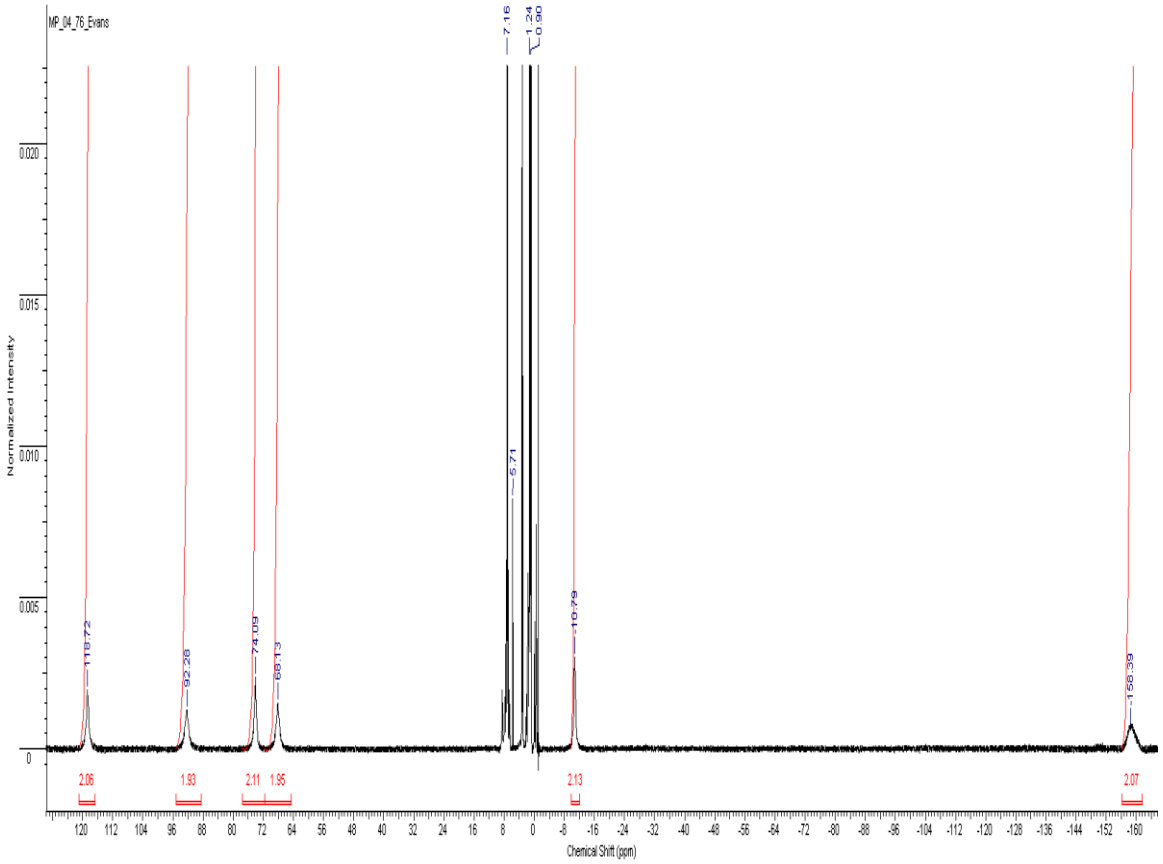

Figure S10. ^{1}H NMR spectrum of **5** in C_6D_6.

8. X-ray crystallography of 5.

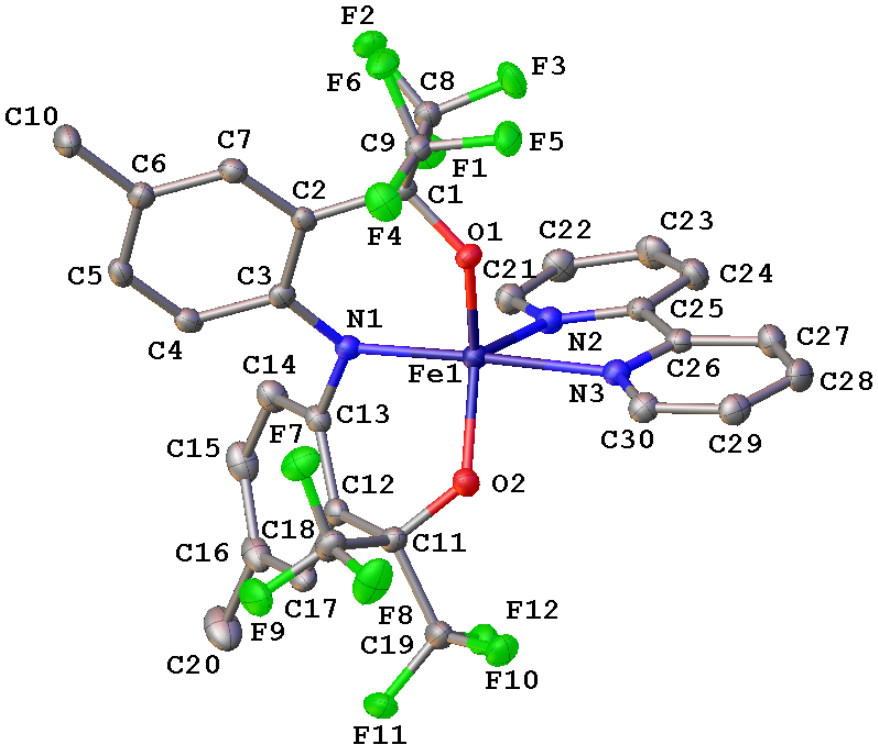

Figure S11. Molecular structure of **5**. Ellipsoids drawn at the 50 % probability level. Hydrogen atoms are omitted for clarity.

X-ray Experimental for 5.

X-Ray Intensity data were collected at 100 K on a Bruker **SMART** diffractometer using MoKα radiation (λ = 0.71073 Å) and an APEXII CCD area detector.

Raw data frames were read by program SAINT and integrated using 3D profiling algorithms. The resulting data were reduced to produce hkl reflections and their intensities and estimated standard deviations. The data were corrected for Lorentz and polarization effects and numerical absorption corrections were applied based on indexed and measured faces.

The structure was solved and refined in SHELXTL6.1, using full-matrix least-squares refinement. The non-H atoms were refined with anisotropic thermal parameters and all of the H atoms were calculated in idealized positions and refined riding on their parent atoms. In the final cycle of refinement, 6926 reflections (of which 5653 are observed with $I > 2\sigma(I)$) were used to refine 435 parameters and the resulting R_1, wR_2 and S (goodness of fit) were 2.91%, 7.74% and 1.071, respectively. The refinement was carried out by minimizing the wR_2 function using F^2 rather than F values. R_1 is calculated to provide a reference to the conventional R value but its function is not minimized.

Table S17. Crystal data and structure refinement for **5**.

Identification code	pasc10	
Empirical formula	$C_{30}H_{20}F_{12}FeN_3O_2$	
Formula weight	738.34	
Temperature	100(2) K	
Wavelength	0.71073 Å	
Crystal system	Monoclinic	
Space group	$P2_1/n$	
Unit cell dimensions	a = 13.5244(6) Å	α = 90°.
	b = 15.9041(7) Å	β = 97.184(2)°.
	c = 14.1139(6) Å	γ = 90°.
Volume	3012.0(2) $Å^3$	
Z	4	
Density (calculated)	1.628 Mg/m^3	
Absorption coefficient	0.609 mm^{-1}	
F(000)	1484	
Crystal size	0.23 x 0.21 x 0.10 mm^3	
Theta range for data collection	1.94 to 27.50°.	
Index ranges	-17≤h≤16, -20≤k≤20, -18≤l≤18	
Reflections collected	49897	
Independent reflections	6926 [R(int) = 0.0463]	
Completeness to theta = 27.50°	100.0 %	
Absorption correction	Numerical	
Max. and min. transmission	0.9404 and 0.8745	
Refinement method	Full-matrix least-squares on F^2	
Data / restraints / parameters	6926 / 0 / 435	
Goodness-of-fit on F^2	1.071	
Final R indices [I>2sigma(I)]	R1 = 0.0291, wR2 = 0.0774 [5653]	
R indices (all data)	R1 = 0.0391, wR2 = 0.0813	
Largest diff. peak and hole	0.400 and -0.343 e.$Å^{-3}$	

$R1 = \Sigma(||F_o| - |F_c||) / \Sigma|F_o|$

$wR2 = [\Sigma[w(F_o^2 - F_c^2)^2] / \Sigma[w(F_o^2)^2]]^{1/2}$

$S = [\Sigma[w(F_o^2 - F_c^2)^2] / (n-p)]^{1/2}$

$w= 1/[\sigma^2(F_o^2)+(m*p)^2+n*p]$, $p = [\max(F_o^2,0)+ 2* F_c^2]/3$, m & n are constants.

Table S18. Atomic coordinates (x 10^4) and equivalent isotropic displacement parameters ($Å^2$x 10^3) for **5**. U(eq) is defined as one third of the trace of the orthogonalized U^{ij} tensor.

Atom	x	y	z	U(eq)
Fe1	4190(1)	6126(1)	2442(1)	16(1)
F1	5655(1)	6079(1)	765(1)	30(1)
F2	6196(1)	7170(1)	95(1)	29(1)
F3	6828(1)	6828(1)	1517(1)	34(1)
F4	4885(1)	8794(1)	1856(1)	29(1)
F5	6267(1)	8226(1)	2435(1)	28(1)
F6	6084(1)	8658(1)	990(1)	29(1)
F7	2088(1)	7388(1)	1941(1)	29(1)
F8	1537(1)	7349(1)	3296(1)	39(1)
F9	638(1)	6868(1)	2050(1)	36(1)
F10	1814(1)	5960(1)	4321(1)	31(1)
F11	541(1)	5629(1)	3326(1)	34(1)
F12	1807(1)	4793(1)	3558(1)	28(1)
O1	5005(1)	7032(1)	2206(1)	19(1)
O2	3037(1)	6124(1)	3080(1)	21(1)
N1	3433(1)	6199(1)	1201(1)	17(1)
N2	5020(1)	4986(1)	2444(1)	19(1)
N3	4987(1)	6045(1)	3861(1)	17(1)
C1	5163(1)	7394(1)	1352(1)	17(1)
C2	4234(1)	7457(1)	595(1)	16(1)
C3	3434(1)	6868(1)	563(1)	16(1)
C4	2600(1)	7017(1)	-128(1)	19(1)
C5	2558(1)	7677(1)	-763(1)	19(1)
C6	3352(1)	8232(1)	-766(1)	19(1)
C7	4176(1)	8105(1)	-77(1)	19(1)
C8	5972(1)	6875(1)	926(1)	22(1)
C9	5600(1)	8277(1)	1650(1)	21(1)
C10	3326(1)	8941(1)	-1477(1)	28(1)
C11	2062(1)	6037(1)	2674(1)	19(1)
C12	1937(1)	5523(1)	1735(1)	18(1)
C13	2621(1)	5616(1)	1064(1)	18(1)
C14	2530(1)	5094(1)	261(1)	23(1)
C15	1768(1)	4510(1)	96(1)	28(1)
C16	1064(1)	4436(1)	725(1)	26(1)
C17	1161(1)	4943(1)	1531(1)	24(1)
C18	1577(1)	6918(1)	2494(1)	25(1)
C19	1542(1)	5604(1)	3470(1)	25(1)
C20	205(1)	3821(1)	558(2)	39(1)

C21	4959(1)	4445(1)	1703(1)	23(1)
C22	5586(1)	3762(1)	1684(1)	26(1)
C23	6319(1)	3638(1)	2451(1)	27(1)
C24	6389(1)	4188(1)	3216(1)	24(1)
C25	5722(1)	4852(1)	3202(1)	18(1)
C26	5691(1)	5445(1)	4014(1)	18(1)
C27	6296(1)	5382(1)	4881(1)	24(1)
C28	6173(1)	5954(1)	5596(1)	25(1)
C29	5434(1)	6560(1)	5440(1)	22(1)
C30	4854(1)	6579(1)	4564(1)	20(1)

Table S19. Bond lengths (Å) for **5**.

Bond	Length (Å)	Bond	Length (Å)
Fe1-O1	1.8689(10)	C1-C9	1.561(2)
Fe1-O2	1.8964(11)	C2-C7	1.396(2)
Fe1-N1	1.9190(12)	C2-C3	1.429(2)
Fe1-N2	2.1324(13)	C3-C4	1.416(2)
Fe1-N3	2.1564(12)	C4-C5	1.376(2)
F1-C8	1.3466(18)	C5-C6	1.391(2)
F2-C8	1.3325(17)	C6-C7	1.399(2)
F3-C8	1.3424(17)	C6-C10	1.506(2)
F4-C9	1.3288(18)	C11-C12	1.549(2)
F5-C9	1.3407(16)	C11-C18	1.556(2)
F6-C9	1.3484(17)	C11-C19	1.558(2)
F7-C18	1.3342(18)	C12-C17	1.400(2)
F8-C18	1.3301(18)	C12-C13	1.412(2)
F9-C18	1.3460(18)	C13-C14	1.398(2)
F10-C19	1.3369(19)	C14-C15	1.385(2)
F11-C19	1.3443(18)	C15-C16	1.385(2)
F12-C19	1.3404(19)	C16-C17	1.388(2)
O1-C1	1.3763(17)	C16-C20	1.515(2)
O2-C11	1.3775(18)	C21-C22	1.380(2)
N1-C3	1.3936(19)	C22-C23	1.388(2)
N1-C13	1.4315(18)	C23-C24	1.383(2)
N2-C21	1.3486(19)	C24-C25	1.388(2)
N2-C25	1.3551(18)	C25-C26	1.488(2)
N3-C30	1.3352(19)	C26-C27	1.388(2)
N3-C26	1.3455(19)	C27-C28	1.384(2)
C1-C2	1.5472(19)	C28-C29	1.386(2)
C1-C8	1.551(2)	C29-C30	1.380(2)

Table S20. Bond angles (°) for **5**.

Bond	Angle (°)	Bond	Angle (°)
O1-Fe1-O2	128.62(5)	F4-C9-C1	110.74(12)
O1-Fe1-N1	92.85(5)	F5-C9-C1	111.21(12)
O2-Fe1-N1	93.27(5)	F6-C9-C1	114.77(12)
O1-Fe1-N2	109.52(5)	O2-C11-C12	113.96(12)
O2-Fe1-N2	117.51(5)	O2-C11-C18	109.84(12)
N1-Fe1-N2	105.86(5)	C12-C11-C18	109.66(12)
O1-Fe1-N3	88.53(4)	O2-C11-C19	103.85(12)
O2-Fe1-N3	84.49(5)	C12-C11-C19	111.96(12)
N1-Fe1-N3	177.75(5)	C18-C11-C19	107.25(12)
N2-Fe1-N3	75.30(5)	C17-C12-C13	117.96(14)
C1-O1-Fe1	129.65(9)	C17-C12-C11	121.49(14)
C11-O2-Fe1	127.16(9)	C13-C12-C11	120.53(13)
C3-N1-C13	117.98(11)	C14-C13-C12	118.84(13)
C3-N1-Fe1	126.37(9)	C14-C13-N1	118.85(13)
C13-N1-Fe1	113.38(9)	C12-C13-N1	122.24(13)
C21-N2-C25	118.77(13)	C15-C14-C13	121.49(15)
C21-N2-Fe1	124.09(10)	C16-C15-C14	120.45(15)
C25-N2-Fe1	116.76(10)	C15-C16-C17	118.27(14)
C30-N3-C26	119.41(13)	C15-C16-C20	122.06(16)
C30-N3-Fe1	123.61(10)	C17-C16-C20	119.67(16)
C26-N3-Fe1	116.88(10)	C16-C17-C12	122.88(15)
O1-C1-C2	115.53(12)	F8-C18-F7	106.79(13)
O1-C1-C8	108.17(12)	F8-C18-F9	106.88(13)
C2-C1-C8	108.50(11)	F7-C18-F9	106.75(12)
O1-C1-C9	103.60(11)	F8-C18-C11	112.74(12)
C2-C1-C9	112.02(12)	F7-C18-C11	111.21(13)
C8-C1-C9	108.77(12)	F9-C18-C11	112.11(13)
C7-C2-C3	119.00(13)	F10-C19-F12	106.50(12)
C7-C2-C1	119.31(12)	F10-C19-F11	106.36(13)
C3-C2-C1	121.70(12)	F12-C19-F11	107.11(13)
N1-C3-C4	120.57(13)	F10-C19-C11	111.31(13)
N1-C3-C2	122.82(12)	F12-C19-C11	110.61(13)
C4-C3-C2	116.53(13)	F11-C19-C11	114.51(12)
C5-C4-C3	122.76(14)	N2-C21-C22	122.60(14)
C4-C5-C6	121.14(13)	C21-C22-C23	118.55(15)
C5-C6-C7	117.02(13)	C24-C23-C22	119.37(15)
C5-C6-C10	121.57(13)	C23-C24-C25	119.36(14)
C7-C6-C10	121.41(14)	N2-C25-C24	121.32(13)
C2-C7-C6	123.45(14)	N2-C25-C26	115.12(13)
F2-C8-F3	107.03(12)	C24-C25-C26	123.52(13)

F2-C8-F1	106.64(12)	N3-C26-C27	121.31(14)
F3-C8-F1	106.52(12)	N3-C26-C25	114.42(12)
F2-C8-C1	113.80(12)	C27-C26-C25	124.22(14)
F3-C8-C1	112.54(12)	C28-C27-C26	118.90(14)
F1-C8-C1	109.89(12)	C27-C28-C29	119.49(14)
F4-C9-F5	106.83(12)	C30-C29-C28	118.35(14)
F4-C9-F6	107.59(12)	N3-C30-C29	122.50(14)
F5-C9-F6	105.25(11)		

Table S21. Anisotropic displacement parameters ($Å^2 x\ 10^3$) for **5**. The anisotropic displacement factor exponent takes the form: $-2\pi^2[h^2\ a^{*2}U^{11} + ... + 2\ h\ k\ a^*\ b^*\ U^{12}]$.

Atom	U_{11}	U_{22}	U_{33}	U_{23}	U_{13}	U_{12}
Fe1	16(1)	18(1)	14(1)	0(1)	2(1)	0(1)
F1	34(1)	25(1)	34(1)	-4(1)	11(1)	5(1)
F2	24(1)	42(1)	22(1)	5(1)	11(1)	5(1)
F3	18(1)	53(1)	29(1)	0(1)	-1(1)	12(1)
F4	30(1)	24(1)	33(1)	-8(1)	1(1)	2(1)
F5	26(1)	32(1)	22(1)	2(1)	-6(1)	-9(1)
F6	29(1)	34(1)	24(1)	6(1)	1(1)	-14(1)
F7	38(1)	20(1)	30(1)	3(1)	12(1)	5(1)
F8	58(1)	37(1)	25(1)	-3(1)	13(1)	20(1)
F9	25(1)	39(1)	42(1)	12(1)	2(1)	12(1)
F10	31(1)	45(1)	19(1)	4(1)	9(1)	7(1)
F11	18(1)	50(1)	34(1)	14(1)	10(1)	5(1)
F12	24(1)	32(1)	29(1)	13(1)	3(1)	1(1)
O1	19(1)	23(1)	14(1)	2(1)	2(1)	-3(1)
O2	17(1)	28(1)	17(1)	0(1)	2(1)	1(1)
N1	15(1)	19(1)	16(1)	-1(1)	2(1)	-2(1)
N2	19(1)	20(1)	17(1)	-1(1)	3(1)	0(1)
N3	18(1)	18(1)	17(1)	0(1)	3(1)	-2(1)
C1	14(1)	20(1)	16(1)	0(1)	3(1)	-1(1)
C2	13(1)	21(1)	15(1)	-3(1)	3(1)	2(1)
C3	17(1)	19(1)	14(1)	-3(1)	4(1)	2(1)
C4	15(1)	23(1)	18(1)	-4(1)	3(1)	-2(1)
C5	15(1)	26(1)	17(1)	-2(1)	0(1)	4(1)
C6	18(1)	22(1)	18(1)	1(1)	4(1)	3(1)
C7	15(1)	22(1)	20(1)	-1(1)	4(1)	0(1)
C8	19(1)	28(1)	18(1)	1(1)	3(1)	2(1)
C9	19(1)	25(1)	18(1)	2(1)	0(1)	-4(1)
C10	21(1)	33(1)	28(1)	10(1)	-2(1)	0(1)
C11	18(1)	24(1)	18(1)	3(1)	5(1)	3(1)
C12	16(1)	19(1)	20(1)	4(1)	1(1)	2(1)
C13	15(1)	17(1)	20(1)	0(1)	0(1)	0(1)
C14	21(1)	24(1)	24(1)	-5(1)	2(1)	2(1)
C15	29(1)	20(1)	32(1)	-7(1)	-5(1)	2(1)
C16	23(1)	18(1)	35(1)	5(1)	-6(1)	-3(1)
C17	20(1)	24(1)	27(1)	9(1)	0(1)	-2(1)
C18	27(1)	28(1)	20(1)	1(1)	7(1)	7(1)
C19	18(1)	33(1)	24(1)	8(1)	4(1)	5(1)
C20	34(1)	27(1)	52(1)	5(1)	-9(1)	-10(1)
C21	23(1)	27(1)	19(1)	-4(1)	2(1)	0(1)

C22	28(1)	26(1)	23(1)	-8(1)	5(1)	1(1)
C23	24(1)	28(1)	30(1)	-4(1)	6(1)	8(1)
C24	19(1)	28(1)	24(1)	-1(1)	0(1)	4(1)
C25	15(1)	22(1)	18(1)	0(1)	4(1)	-2(1)
C26	16(1)	20(1)	18(1)	1(1)	3(1)	-2(1)
C27	20(1)	26(1)	24(1)	-1(1)	-2(1)	2(1)
C28	24(1)	32(1)	18(1)	-2(1)	-3(1)	-3(1)
C29	26(1)	21(1)	20(1)	-4(1)	3(1)	-4(1)
C30	23(1)	17(1)	21(1)	-1(1)	3(1)	-1(1)

9. Synthesis of 5.H_2O.

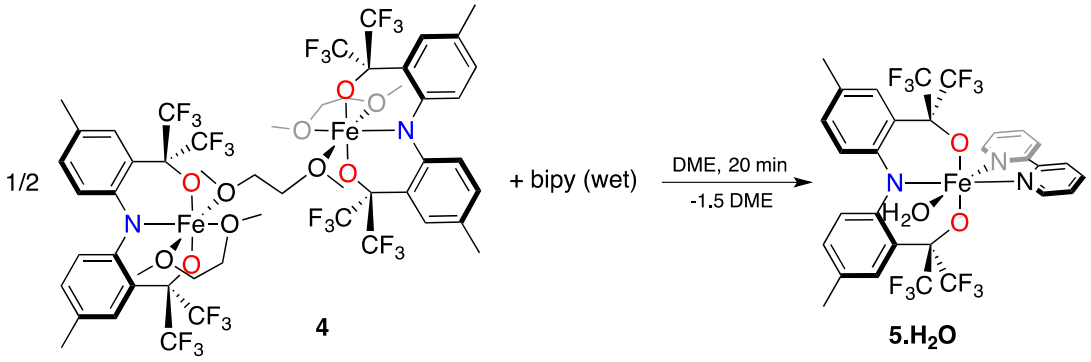

Figure S12. Synthesis of **5.H_2O**.

The preparation of **5.H_2O** follows the same method as complex **5**, however, wet 2,2'-bipyridine that was not previously recrystallized is used. Yield: 65.7 %. ^{1}H-NMR (C_6D_6, 300 MHz, 25 °C): δ = 120.14 ($\nu_{1/2}$ = 840 Hz), 94.72 ($\nu_{1/2}$ = 840 Hz), 74.62 ($\nu_{1/2}$ = 600 Hz), 69.85 (720 Hz), -11.11 ($\nu_{1/2}$ = 360 Hz), -93.18 ($\nu_{1/2}$ = 1200 Hz).

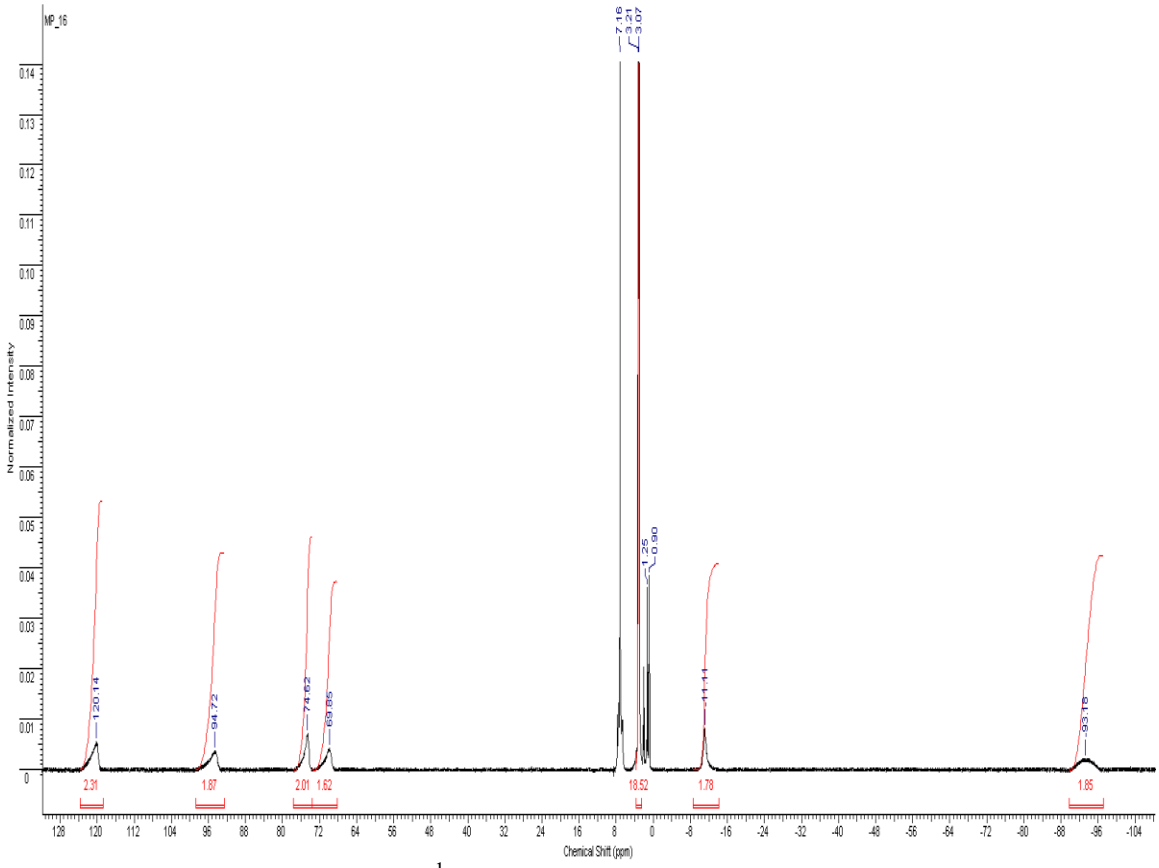

Figure S13. ^{1}H NMR spectrum of **5.H_2O** in C_6D_6.

10. X-ray crystallography of 5.H_2O.

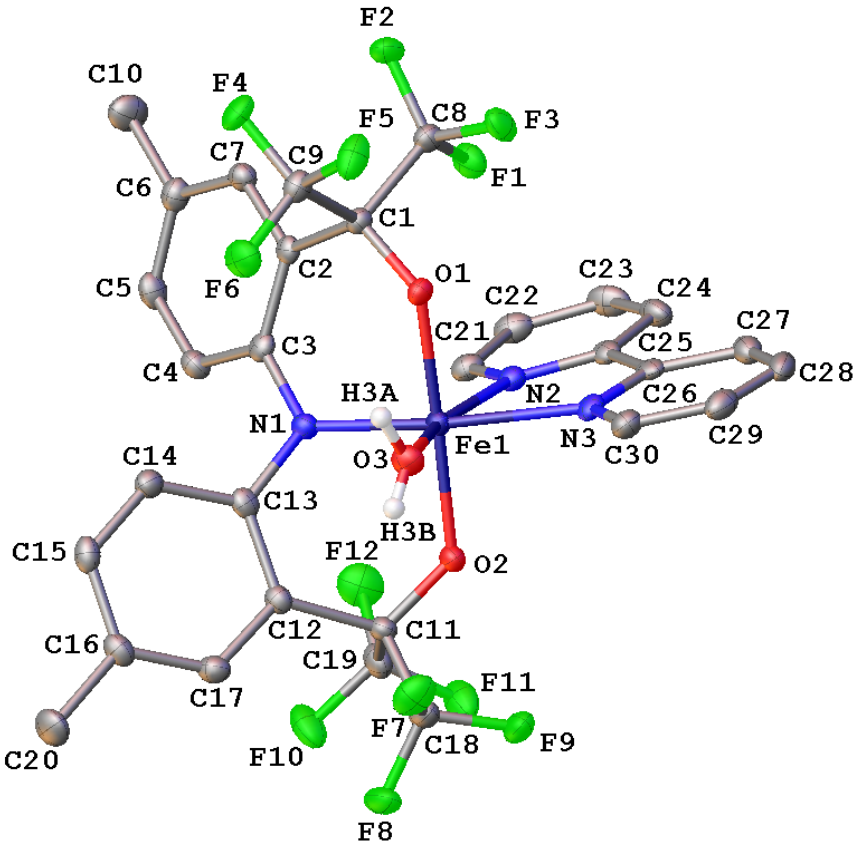

Figure S14. Molecular structure of **5.H_2O**. Ellipsoids drawn at the 50 % probability level. Arene and methyl group hydrogen atoms and solvent molecules were removed for clarity.

X-ray experimental for 5.H_2O.

X-Ray Intensity data were collected at 100 K on a Bruker **SMART** diffractometer using MoKα radiation (λ = 0.71073 Å) and an APEXII CCD area detector.

Raw data frames were read by program SAINT[1] and integrated using 3D profiling algorithms. The resulting data were reduced to produce hkl reflections and their intensities and estimated standard deviations. The data were corrected for Lorentz and polarization effects and numerical absorption corrections were applied based on indexed and measured faces.

The structure was solved and refined in SHELXTL2013, using full-matrix least-squares refinement. The non-H atoms were refined with anisotropic thermal parameters and all of the H atoms were calculated in idealized positions and refined riding on their parent atoms. The asymmetric unit consists of the Fe complex and two DME solvent molecules. One of the solvent molecules has its bridging Carbon atoms and C34 methyl group disordered and refined in two parts with their site occupation factors dependently refined. The coordinated water molecule has its protons obtained from a Difference Fourier map and refined freely. Both of the protons are hydrogen bonded to the two oxygen atoms of the disordered DME solvent molecule. In the final cycle of refinement, 9511 reflections (of which 7064 are observed with $I > 2\sigma(I)$) were used to refine 563 parameters and the resulting R_1, wR_2 and S (goodness of fit) were 3.80%, 8.79% and 0.955, respectively. The refinement was carried out by minimizing the wR_2 function using F^2 rather than F values. R_1 is calculated to provide a reference to the conventional R value but its function is not minimized.

Table S22. Crystal data and structure refinement for **5.H_2O**.

Identification code	pasc9	
Empirical formula	C38 H42 F12 Fe N3 O7	
Formula weight	936.59	
Temperature	100(2) K	
Wavelength	0.71073 Å	
Crystal system	Triclinic	
Space group	P -1	
Unit cell dimensions	a = 11.3312(3) Å	α= 104.924(2)°.
	b = 11.9100(3) Å	β= 102.833(2)°.
	c = 17.0755(5) Å	γ = 103.035(2)°.
Volume	2070.99(10) $Å^3$	
Z	2	
Density (calculated)	1.502 Mg/m^3	
Absorption coefficient	0.469 mm^{-1}	
F(000)	962	
Crystal size	0.403 x 0.226 x 0.176 mm^3	
Theta range for data collection	1.855 to 27.500°.	
Index ranges	-14≤h≤14, -15≤k≤15, -22≤l≤22	
Reflections collected	48219	
Independent reflections	9511 [R(int) = 0.0602]	
Completeness to theta = 25.242°	100.0 %	
Absorption correction	Analytical	
Max. and min. transmission	0.9447 and 0.8782	
Refinement method	Full-matrix least-squares on F^2	
Data / restraints / parameters	9511 / 0 / 563	
Goodness-of-fit on F^2	0.955	
Final R indices [I>2sigma(I)]	R1 = 0.0380, wR2 = 0.0879 [7064]	
R indices (all data)	R1 = 0.0556, wR2 = 0.0942	
Extinction coefficient	n/a	
Largest diff. peak and hole	0.479 and -0.402 $e.Å^{-3}$	

$R1 = \Sigma(||F_o| - |F_c||) / \Sigma|F_o|$

$wR2 = [\Sigma[w(F_o^2 - F_c^2)^2] / \Sigma[w(F_o^2)^2]]^{1/2}$

$S = [\Sigma[w(F_o^2 - F_c^2)^2] / (n-p)]^{1/2}$

$w= 1/[\sigma^2(F_o^2)+(m*p)^2+n*p]$, $p = [\max(F_o^2,0)+ 2* F_c^2]/3$, m & n are constants.

Table S23. Atomic coordinates (x 10^4) and equivalent isotropic dispacement parameters ($Å^2$x 10^3) for **5.H_2O**. U(eq) is defined as one third of the trace of the orthogonalized U^{ij} tensor.

Atom	x	y	Z	U(eq)
Fe1	5333(1)	2375(1)	2168(1)	12(1)
F1	5375(1)	-427(1)	3031(1)	23(1)
F2	4633(1)	-342(1)	4096(1)	23(1)
F3	3422(1)	-518(1)	2891(1)	24(1)
F4	4544(1)	1869(1)	4964(1)	22(1)
F5	2984(1)	1498(1)	3860(1)	28(1)
F6	4493(1)	3187(1)	4312(1)	27(1)
F7	5246(1)	5183(1)	1207(1)	32(1)
F8	7062(1)	5967(1)	1056(1)	32(1)
F9	5959(1)	4141(1)	300(1)	29(1)
F10	9093(1)	5473(1)	1990(1)	32(1)
F11	8221(1)	3845(1)	911(1)	31(1)
F12	8667(1)	3720(1)	2173(1)	33(1)
O1	4509(1)	1582(1)	2832(1)	14(1)
O2	6104(1)	3242(1)	1514(1)	16(1)
O3	4034(1)	3423(1)	2204(1)	19(1)
O4	3590(2)	5728(1)	2352(1)	36(1)
O5	2701(2)	4234(1)	3304(1)	34(1)
O6	-343(1)	7358(1)	-184(1)	35(1)
O7	195(1)	9208(2)	1380(1)	36(1)
N1	6670(1)	3432(1)	3200(1)	14(1)
N2	6160(2)	910(1)	1818(1)	14(1)
N3	3907(1)	999(1)	1038(1)	15(1)
C1	4969(2)	1443(2)	3602(1)	13(1)
C2	6408(2)	2050(2)	4061(1)	13(1)
C3	7142(2)	3016(2)	3872(1)	14(1)
C4	8440(2)	3512(2)	4340(1)	17(1)
C5	8985(2)	3124(2)	4988(1)	19(1)
C6	8265(2)	2202(2)	5198(1)	19(1)
C7	7001(2)	1682(2)	4728(1)	16(1)
C8	4601(2)	37(2)	3415(1)	16(1)
C9	4248(2)	1996(2)	4190(1)	17(1)
C10	8833(2)	1779(2)	5919(1)	28(1)
C11	6889(2)	4412(2)	1770(1)	15(1)
C12	7058(2)	5214(2)	2686(1)	15(1)
C13	7005(2)	4693(2)	3341(1)	15(1)
C14	7198(2)	5492(2)	4159(1)	16(1)
C15	7475(2)	6738(2)	4337(1)	18(1)

C16	7546(2)	7258(2)	3699(1)	19(1)
C17	7331(2)	6481(2)	2891(1)	18(1)
C18	6297(2)	4942(2)	1087(1)	22(1)
C19	8221(2)	4372(2)	1710(1)	22(1)
C20	7830(2)	8616(2)	3889(1)	27(1)
C21	7326(2)	943(2)	2236(1)	18(1)
C22	7779(2)	-58(2)	2065(1)	22(1)
C23	7005(2)	-1111(2)	1432(1)	26(1)
C24	5808(2)	-1152(2)	991(1)	22(1)
C25	5405(2)	-123(2)	1193(1)	15(1)
C26	4145(2)	-68(2)	752(1)	16(1)
C27	3271(2)	-1038(2)	72(1)	21(1)
C28	2110(2)	-914(2)	-296(1)	23(1)
C29	1855(2)	173(2)	1(1)	22(1)
C30	2781(2)	1104(2)	663(1)	19(1)
C31	3534(3)	6543(2)	1892(2)	48(1)
C35	-1200(2)	6334(2)	-868(2)	44(1)
C36	-198(2)	7134(2)	597(2)	41(1)
C37	708(2)	8219(2)	1302(2)	37(1)
C38	1007(2)	10268(2)	2046(2)	43(1)
C32	3294(6)	6232(4)	3150(3)	34(1)
C33	3546(4)	5469(4)	3702(3)	30(1)
C34	1522(5)	4075(5)	3346(3)	39(1)
C32'	3831(7)	6148(5)	3234(4)	39(2)
C33'	2725(6)	5507(5)	3451(4)	36(2)
C34'	1507(5)	3584(6)	3405(4)	34(1)

Table S24. Bond lengths (Å) for **5.H_2O**.

Bond	Length (Å)	Bond	Length (Å)
Fe1-O1	1.9174(13)	N2-C25	1.352(2)
Fe1-O2	1.9230(13)	N3-C30	1.344(2)
Fe1-N1	1.9491(15)	N3-C26	1.349(2)
Fe1-O3	2.1350(15)	C1-C9	1.542(3)
Fe1-N2	2.1746(15)	C1-C2	1.551(2)
Fe1-N3	2.1930(15)	C1-C8	1.558(2)
F1-C8	1.339(2)	C2-C7	1.411(2)
F2-C8	1.347(2)	C2-C3	1.414(3)
F3-C8	1.338(2)	C3-C4	1.411(3)
F4-C9	1.345(2)	C4-C5	1.382(3)
F5-C9	1.344(2)	C5-C6	1.389(3)
F6-C9	1.333(2)	C6-C7	1.384(3)
F7-C18	1.332(2)	C6-C10	1.515(3)
F8-C18	1.349(2)	C11-C19	1.546(3)
F9-C18	1.345(2)	C11-C12	1.553(3)
F10-C19	1.344(2)	C11-C18	1.558(3)
F11-C19	1.346(2)	C12-C17	1.402(2)
F12-C19	1.342(2)	C12-C13	1.418(3)
O1-C1	1.369(2)	C13-C14	1.409(3)
O2-C11	1.370(2)	C14-C15	1.382(3)
O3-H3A	0.86(3)	C15-C16	1.393(3)
O3-H3B	0.76(3)	C16-C17	1.383(3)
O4-C32'	1.400(6)	C16-C20	1.508(3)
O4-C31	1.402(3)	C21-C22	1.390(3)
O4-C32	1.483(5)	C22-C23	1.376(3)
O5-C34	1.328(5)	C23-C24	1.381(3)
O5-C33	1.449(4)	C24-C25	1.391(3)
O5-C33'	1.464(5)	C25-C26	1.483(3)
O5-C34'	1.471(6)	C26-C27	1.394(3)
O6-C36	1.408(3)	C27-C28	1.385(3)
O6-C35	1.422(3)	C28-C29	1.383(3)
O7-C37	1.416(3)	C29-C30	1.382(3)
O7-C38	1.416(3)	C36-C37	1.492(3)
N1-C13	1.405(2)	C32-C33	1.496(7)
N1-C3	1.409(2)	C32'-C33'	1.487(9)
N2-C21	1.341(2)		

Table S25. Bond angles (°) for **5.H_2O**.

Bond	Angle (°)	Bond	Angle (°)
O1-Fe1-O2	176.47(5)	F2-C8-C1	115.89(15)
O1-Fe1-N1	89.55(6)	F6-C9-F5	106.95(15)
O2-Fe1-N1	90.31(6)	F6-C9-F4	106.74(15)
O1-Fe1-O3	86.48(6)	F5-C9-F4	105.97(16)
O2-Fe1-O3	90.05(6)	F6-C9-C1	110.23(16)
N1-Fe1-O3	98.11(6)	F5-C9-C1	112.17(15)
O1-Fe1-N2	90.92(6)	F4-C9-C1	114.34(15)
O2-Fe1-N2	92.59(6)	O2-C11-C19	108.77(15)
N1-Fe1-N2	99.24(6)	O2-C11-C12	116.10(16)
O3-Fe1-N2	162.43(6)	C19-C11-C12	107.34(15)
O1-Fe1-N3	87.34(5)	O2-C11-C18	103.53(14)
O2-Fe1-N3	93.19(5)	C19-C11-C18	108.55(16)
N1-Fe1-N3	172.95(6)	C12-C11-C18	112.33(15)
O3-Fe1-N3	88.02(6)	C17-C12-C13	118.58(17)
N2-Fe1-N3	74.50(6)	C17-C12-C11	120.28(17)
C1-O1-Fe1	131.71(11)	C13-C12-C11	121.07(16)
C11-O2-Fe1	129.22(11)	N1-C13-C14	119.13(17)
Fe1-O3-H3A	119.2(16)	N1-C13-C12	123.38(17)
Fe1-O3-H3B	128(2)	C14-C13-C12	117.27(17)
H3A-O3-H3B	105(2)	C15-C14-C13	122.41(18)
C32'-O4-C31	119.7(3)	C14-C15-C16	120.65(18)
C31-O4-C32	108.0(2)	C17-C16-C15	117.45(17)
C34-O5-C33	115.7(3)	C17-C16-C20	121.80(18)
C33'-O5-C34'	107.3(3)	C15-C16-C20	120.75(18)
C36-O6-C35	111.55(19)	C16-C17-C12	123.61(18)
C37-O7-C38	112.13(18)	F7-C18-F9	106.62(17)
C13-N1-C3	118.41(15)	F7-C18-F8	107.32(16)
C13-N1-Fe1	117.89(11)	F9-C18-F8	105.02(16)
C3-N1-Fe1	122.67(12)	F7-C18-C11	110.54(16)
C21-N2-C25	119.08(16)	F9-C18-C11	111.39(15)
C21-N2-Fe1	123.45(13)	F8-C18-C11	115.43(17)
C25-N2-Fe1	117.21(12)	F12-C19-F10	106.60(16)
C30-N3-C26	118.19(16)	F12-C19-F11	106.42(16)
C30-N3-Fe1	124.83(13)	F10-C19-F11	106.01(16)
C26-N3-Fe1	116.70(12)	F12-C19-C11	110.43(16)
O1-C1-C9	107.06(14)	F10-C19-C11	114.04(16)
O1-C1-C2	116.80(15)	F11-C19-C11	112.84(16)
C9-C1-C2	107.51(15)	N2-C21-C22	122.43(19)
O1-C1-C8	104.51(14)	C23-C22-C21	118.40(19)
C9-C1-C8	109.62(15)	C22-C23-C24	119.74(19)

C2-C1-C8	111.16(14)	C23-C24-C25	119.24(19)
C7-C2-C3	118.17(16)	N2-C25-C24	121.10(18)
C7-C2-C1	119.22(16)	N2-C25-C26	115.39(16)
C3-C2-C1	122.51(15)	C24-C25-C26	123.51(17)
N1-C3-C4	118.89(17)	N3-C26-C27	121.85(18)
N1-C3-C2	123.34(16)	N3-C26-C25	115.48(16)
C4-C3-C2	117.56(16)	C27-C26-C25	122.65(18)
C5-C4-C3	122.44(18)	C28-C27-C26	118.82(19)
C4-C5-C6	120.56(18)	C29-C28-C27	119.57(18)
C7-C6-C5	117.64(17)	C30-C29-C28	118.25(19)
C7-C6-C10	120.75(18)	N3-C30-C29	123.28(19)
C5-C6-C10	121.61(17)	O6-C36-C37	110.5(2)
C6-C7-C2	123.56(18)	O7-C37-C36	109.26(19)
F3-C8-F1	106.68(15)	O4-C32-C33	108.2(4)
F3-C8-F2	105.31(15)	O5-C33-C32	110.6(4)
F1-C8-F2	106.72(14)	O4-C32'-C33'	108.6(5)
F3-C8-C1	111.50(14)	O5-C33'-C32'	108.5(5)
F1-C8-C1	110.21(15)		

Table S26. Anisotropic displacement parameters ($Å^2 x\ 10^3$) for **5.H_2O**. The anisotropic displacement factor exponent takes the form: $-2\pi^2[h^2\ a^{*2}U^{11} + ... + 2\ h\ k\ a^*\ b^*\ U^{12}]$.

Atom	U_{11}	U_{22}	U_{33}	U_{23}	U_{13}	U_{12}
Fe1	15(1)	11(1)	12(1)	3(1)	4(1)	4(1)
F1	27(1)	16(1)	28(1)	4(1)	12(1)	10(1)
F2	30(1)	20(1)	20(1)	12(1)	5(1)	4(1)
F3	19(1)	17(1)	26(1)	6(1)	-2(1)	-1(1)
F4	26(1)	33(1)	12(1)	8(1)	7(1)	13(1)
F5	15(1)	44(1)	19(1)	2(1)	5(1)	9(1)
F6	38(1)	20(1)	28(1)	6(1)	14(1)	16(1)
F7	37(1)	40(1)	27(1)	17(1)	10(1)	24(1)
F8	57(1)	16(1)	27(1)	11(1)	19(1)	6(1)
F9	50(1)	22(1)	15(1)	7(1)	9(1)	9(1)
F10	25(1)	23(1)	40(1)	-2(1)	16(1)	-3(1)
F11	33(1)	26(1)	32(1)	0(1)	21(1)	5(1)
F12	25(1)	38(1)	45(1)	17(1)	12(1)	18(1)
O1	14(1)	16(1)	11(1)	5(1)	2(1)	3(1)
O2	21(1)	11(1)	15(1)	4(1)	5(1)	2(1)
O3	24(1)	16(1)	21(1)	7(1)	7(1)	10(1)
O4	54(1)	22(1)	28(1)	3(1)	10(1)	10(1)
O5	40(1)	30(1)	35(1)	7(1)	16(1)	13(1)
O6	29(1)	34(1)	34(1)	10(1)	4(1)	2(1)
O7	25(1)	50(1)	28(1)	7(1)	1(1)	14(1)
N1	16(1)	13(1)	13(1)	4(1)	5(1)	4(1)
N2	18(1)	13(1)	14(1)	6(1)	7(1)	5(1)
N3	16(1)	17(1)	12(1)	5(1)	7(1)	4(1)
C1	13(1)	14(1)	12(1)	5(1)	3(1)	5(1)
C2	14(1)	13(1)	12(1)	2(1)	4(1)	5(1)
C3	16(1)	15(1)	12(1)	3(1)	6(1)	7(1)
C4	16(1)	14(1)	20(1)	4(1)	4(1)	2(1)
C5	14(1)	18(1)	21(1)	3(1)	-1(1)	4(1)
C6	20(1)	19(1)	17(1)	5(1)	3(1)	9(1)
C7	18(1)	15(1)	17(1)	6(1)	5(1)	5(1)
C8	17(1)	16(1)	14(1)	6(1)	4(1)	5(1)
C9	18(1)	20(1)	14(1)	4(1)	4(1)	7(1)
C10	22(1)	32(1)	28(1)	15(1)	-1(1)	8(1)
C11	19(1)	12(1)	15(1)	5(1)	7(1)	5(1)
C12	15(1)	13(1)	16(1)	4(1)	5(1)	4(1)
C13	12(1)	14(1)	17(1)	4(1)	3(1)	4(1)
C14	16(1)	18(1)	15(1)	6(1)	4(1)	5(1)
C15	16(1)	17(1)	18(1)	-1(1)	3(1)	6(1)
C16	18(1)	12(1)	24(1)	4(1)	6(1)	5(1)

C17	22(1)	16(1)	21(1)	8(1)	8(1)	6(1)
C18	35(1)	15(1)	18(1)	7(1)	10(1)	7(1)
C19	23(1)	16(1)	24(1)	2(1)	9(1)	2(1)
C20	41(1)	14(1)	28(1)	4(1)	11(1)	11(1)
C21	19(1)	22(1)	18(1)	9(1)	9(1)	9(1)
C22	25(1)	26(1)	26(1)	14(1)	14(1)	15(1)
C23	34(1)	21(1)	37(1)	15(1)	22(1)	18(1)
C24	32(1)	14(1)	24(1)	6(1)	14(1)	6(1)
C25	22(1)	14(1)	14(1)	5(1)	11(1)	6(1)
C26	22(1)	16(1)	13(1)	7(1)	10(1)	4(1)
C27	26(1)	16(1)	17(1)	3(1)	10(1)	1(1)
C28	24(1)	23(1)	13(1)	3(1)	4(1)	-4(1)
C29	18(1)	29(1)	18(1)	9(1)	4(1)	2(1)
C30	21(1)	22(1)	16(1)	8(1)	6(1)	6(1)
C31	73(2)	28(1)	51(2)	17(1)	26(2)	23(1)
C35	33(1)	32(1)	53(2)	1(1)	3(1)	7(1)
C36	39(2)	44(2)	48(2)	26(1)	18(1)	12(1)
C37	31(1)	59(2)	34(1)	27(1)	12(1)	22(1)
C38	29(1)	59(2)	30(1)	6(1)	3(1)	9(1)

11. Cyclic Voltammetry of 3-5.

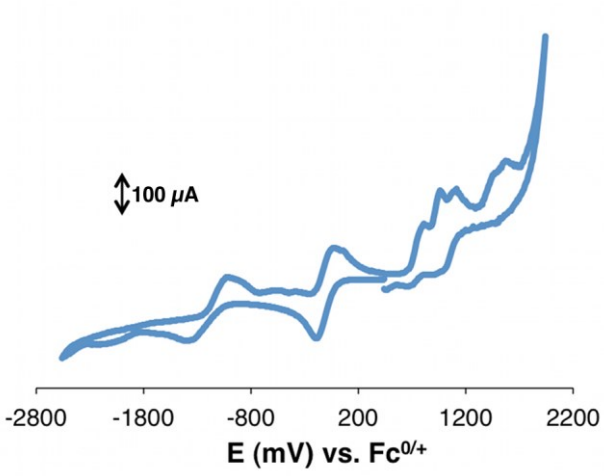

Figure S15. Cyclic voltammogram of **3** in acetonitrile using 0.1 M Bu_4NPF_6 as supporting electrolyte and a scan rate of 100 mV/s. Working electrode: 3 mm glassy carbon. Reference electrode: Ag/AgCl. Auxiliary electrode: Pt wire.

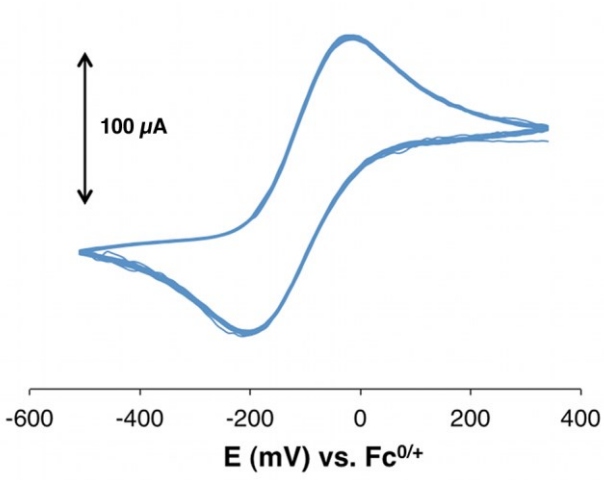

Figure S16. Cyclic voltammogram of **3**: 20 scans at 100 mV/s.

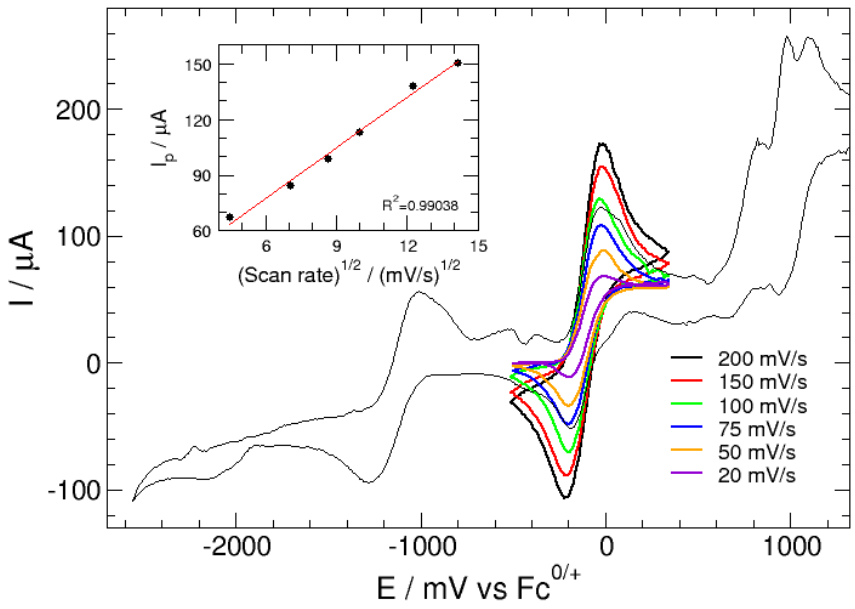

Figure S17. Cyclic voltammogram of **3**: scan rate dependence of the signal with $E_{1/2}$ = 110 mV (ΔE_p = 170 – 200 mV). Inset depicts the linear dependence of I_p vs. (scan rate)$^{1/2}$.

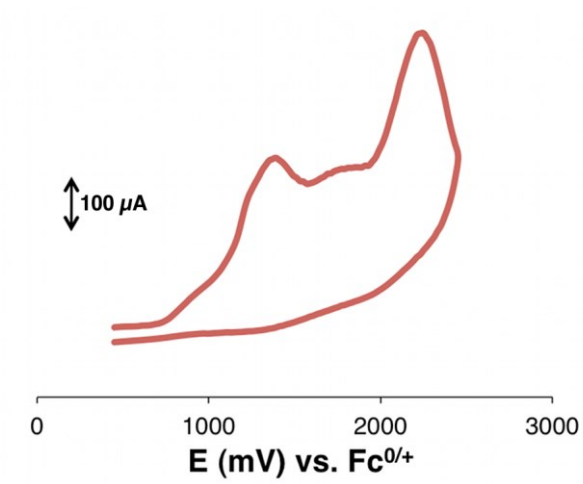

Figure S18. Cyclic voltammogram of **4** in acetonitrile using 0.1 M Bu_4NPF_6 as supporting electrolyte and a scan rate of 200 mV/s. Working electrode: 3 mm glassy carbon. Reference electrode: Ag/AgCl. Auxiliary electrode: Pt wire.

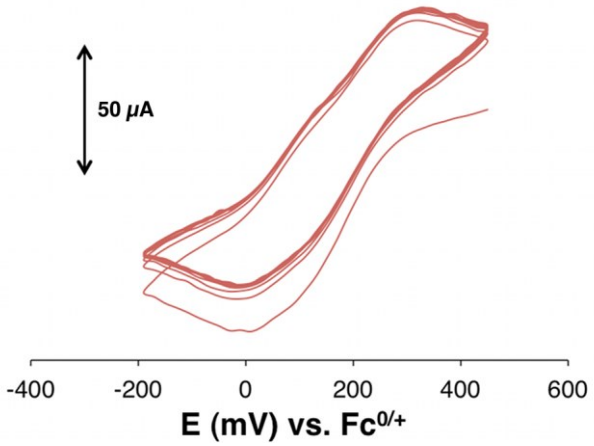

Figure S19. Cyclic voltammogram of **4**: 15 scans at 200 mV/s.

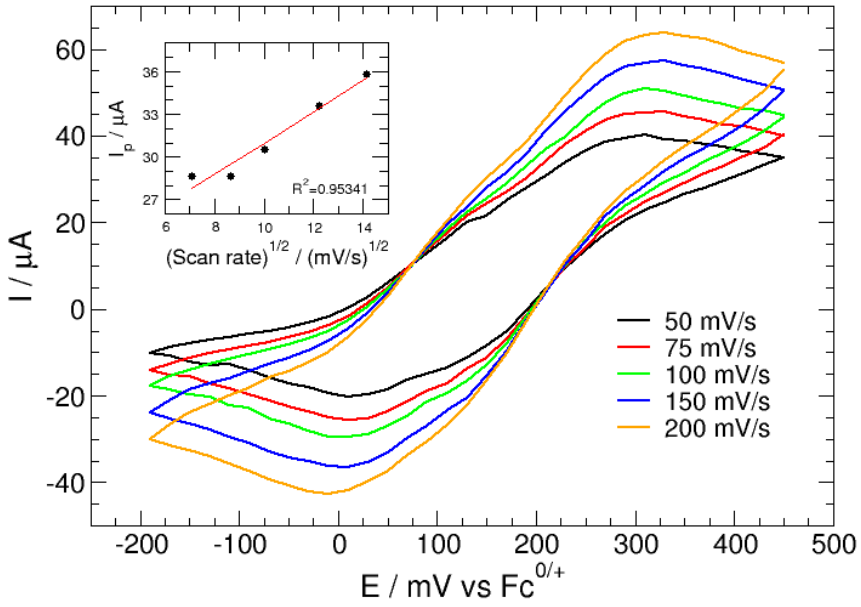

Figure S20. Cyclic voltammogram of **4**: scan rate dependence of the signal with $E_{1/2}$ = 160 mV (ΔE_p = 300 – 340 mV). Inset depicts the linear dependence of I_p vs. (scan rate)$^{1/2}$.

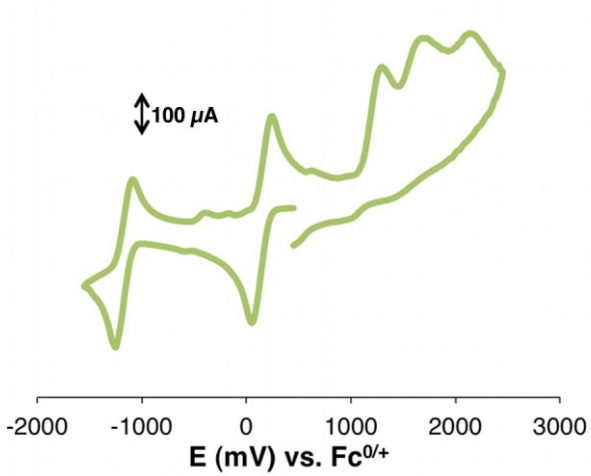

Figure S21. Cyclic voltammogram of **5** in acetonitrile using 0.1 M Bu_4NPF_6 as supporting electrolyte and a scan rate of 400 mV/s. Working electrode: 3 mm glassy carbon. Reference electrode: Ag/AgCl. Auxiliary electrode: Pt wire.

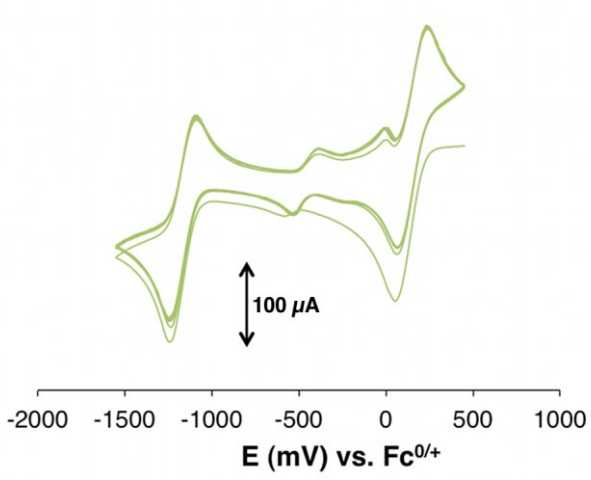

Figure S22. Cyclic voltammogram of **5**: 15 scans at 200 mV/s.

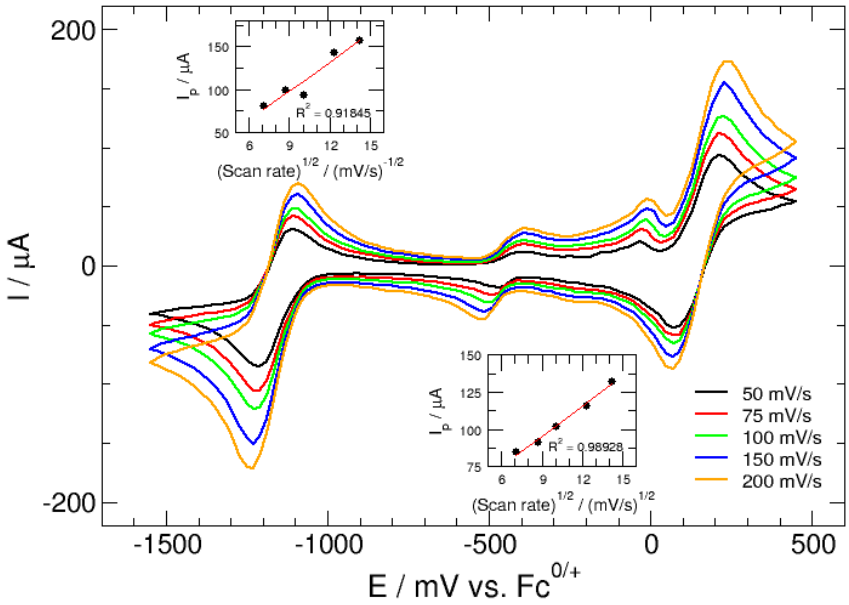

Figure S23. Cyclic voltammogram of **5**: scan rate dependence of the signals with $E_{1/2}$ = 150 mV (ΔE_p = 135 – 170 mV) and -1165 mV (ΔE_p = 110 – 150 mV). Insets depict the linear dependence of I_p vs. (scan rate)$^{1/2}$.

12. DFT Calculations of 3 and 5.

Spin-unrestricted DFT calculations were carried out at the B3LYP level of theory[1, 2] using Gaussian 09.[3] The LANL2DZ basis set and an effective core potential were used for the Fe atoms, and 6-31G** was used for all other atoms. Initial geometries were derived from the corresponding crystal structures (**3'** corresponds to **3** after removing solvent molecules and counterions), and subjected to optimization. Normal mode analysis was performed to verify the absence of negative eigenvalues. MO analysis was performed using the biorthogonal corresponding orbital approach as implemented in Gaussian 09.

Table S27 summarizes the values of relevant distances and angles in the optimized geometries and compares them to the experimentally determined values. Bond lengths differ less than 0.10 Å from the values observed in the corresponding crystal structures.

Table S27. Comparison between selected experimental and calculated bond lengths (Å) and angles (°).

3/3'			**5/5'**		
Parameter	**Experimental**	**Calculated**	**Parameter**	**Experimental**	**Calculated**
Fe1-Cl1	2.3100(11)	2.3967	**Fe1-N1**	1.9190(12)	2.0132
Fe1-Cl2	2.4252(15)	2.3967	**Fe1-N2**	2.1324(13)	2.2154
Fe1-N1	1.926(4)	2.0837	**Fe1-N3**	2.1564(12)	2.2491
Fe1-O1	1.980(3)	1.9203	**Fe1-O1**	1.86899(10)	1.8772
Fe1-O2	1.973(3)	1.9203	**Fe1-O2**	1.8964(11)	1.9022
O1-Fe1-O2	155.72(14)	167.87	**O1-Fe1-O2**	128.62(5)	142.01
τ	0.22	0.74	**τ**	0.82	0.60

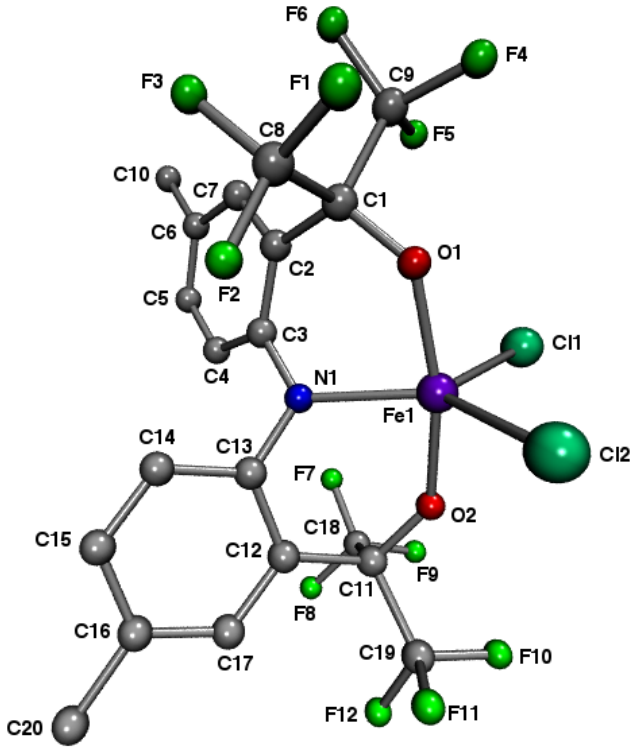

Figure S24. Optimized geometry of **3'**.

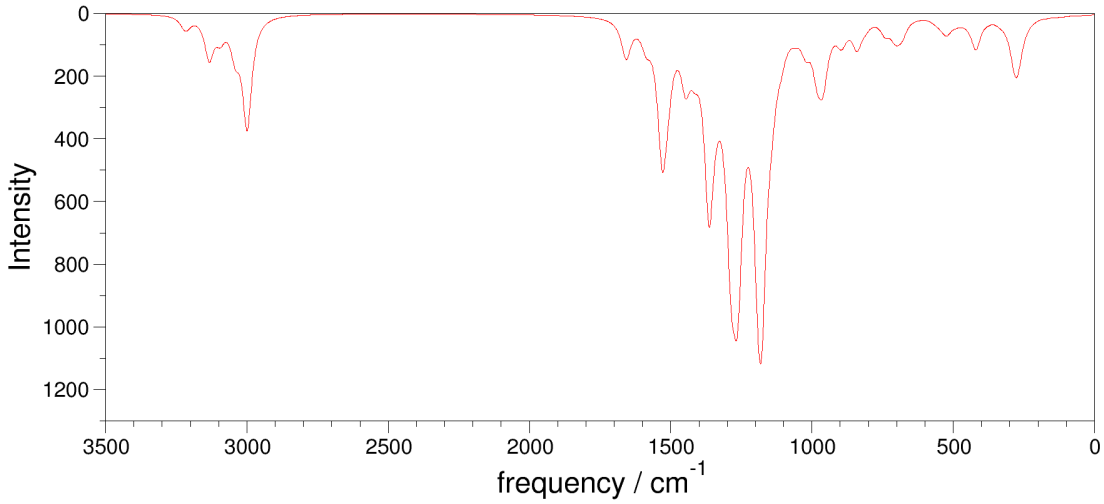

Figure S25. Calculated gaussian IR spectrum for **3'.**

Table S28. Atomic coordinates for the optimized geometry of **3'**.

Atom	x	y	z
Fe1	-0.000008	-1.547603	-0.000006
N1	0.000001	0.536101	-0.000034
O1	-1.853715	-1.344739	-0.458401
O2	1.853699	-1.344753	0.458378
C1	-2.793676	-0.373589	-0.411572
C2	-2.419225	0.853903	0.447231
C3	-1.053998	1.243559	0.555231
C4	-0.780742	2.399578	1.339916
C5	-1.77807	3.144823	1.943078
C6	-3.126099	2.781289	1.81069
C7	-3.406454	1.639681	1.058305
C8	-3.077413	0.128303	-1.868772
C9	-4.093034	-1.083818	0.116701
C10	-4.227582	3.574891	2.474373
C11	2.793668	-0.373607	0.411565
C12	2.41924	0.853887	-0.447243
C13	1.054022	1.243552	-0.555269
C14	0.780786	2.399572	-1.339963
C15	1.778127	3.144811	-1.943105
C16	3.126155	2.781271	-1.810685
C17	3.406487	1.639662	-1.058297
C18	3.077383	0.12828	1.868771
C19	4.09303	-1.083844	-0.116687
C20	4.227657	3.574899	-2.474305
Cl1	-0.456257	-2.866361	1.948507
Cl2	0.456223	-2.866398	-1.948498
F1	-3.507276	-0.861887	-2.680157
F2	-1.96807	0.649418	-2.422847
F3	-4.029827	1.105305	-1.921463
F4	-4.286067	-2.267154	-0.487181
F5	-4.020534	-1.308416	1.439573
F6	-5.255574	-0.376747	-0.092807
F7	1.968033	0.649399	2.422827
F8	4.0298	1.105277	1.921479
F9	3.507228	-0.861914	2.680161
F10	4.020552	-1.308433	-1.439563
F11	4.286045	-2.267185	0.487189
F12	5.255571	-0.376782	0.092844

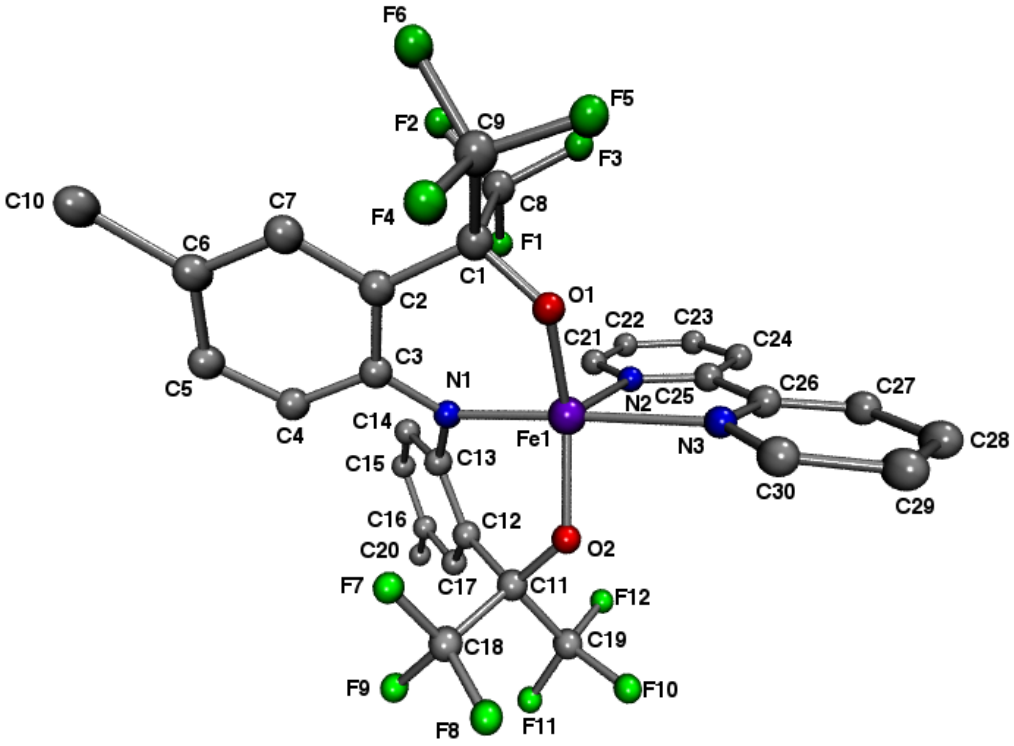

Figure S26. Optimized geometry of **5**.

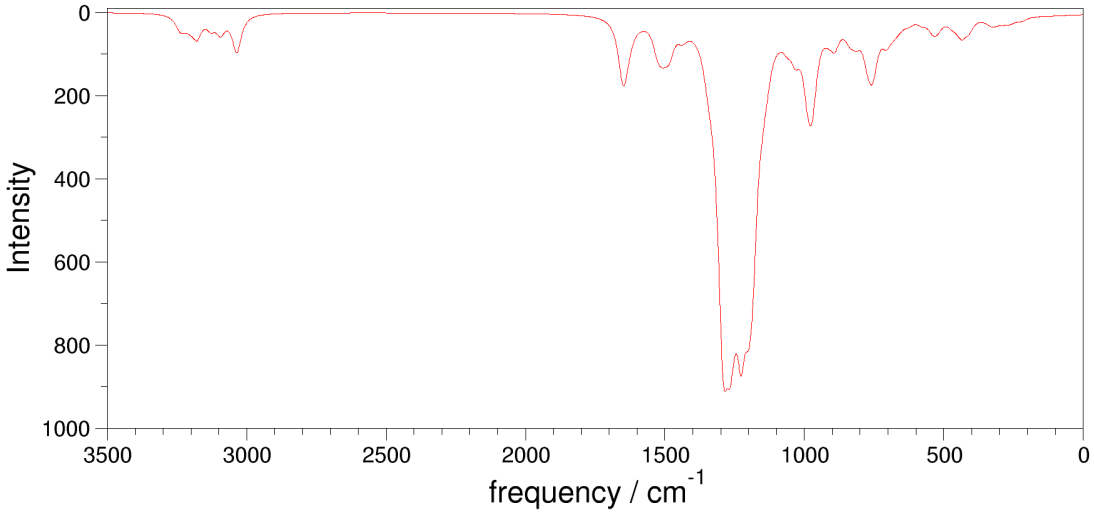

Figure S27. Calculated gaussian IR spectrum for **5**.

Table S29. Atomic coordinates for the optimized geometry of **5**.

Atom	x	y	z
Fe1	-0.036054	0.75638	-0.258562
N1	0.214607	-1.15144	0.333329
N2	-0.61711	1.923388	1.529118
N3	-0.371201	2.866227	-0.961818
O1	1.81124	0.930827	-0.542914
O2	-1.649179	0.268387	-1.140589
C1	2.872709	0.190165	-0.109038
C2	2.641518	-1.340157	-0.116776
C3	1.345962	-1.915315	0.104295
C4	1.235301	-3.330789	0.004828
C5	2.328002	-4.144393	-0.226052
C6	3.609356	-3.595014	-0.361702
C7	3.725634	-2.201611	-0.305835
C8	3.231343	0.621379	1.349153
C9	4.047186	0.616726	-1.06072
C10	4.821832	-4.470221	-0.55583
C11	-2.446373	-0.830593	-0.992022
C12	-2.226945	-1.621735	0.326363
C13	-0.930447	-1.764425	0.887792
C14	-0.79114	-2.471749	2.101915
C15	-1.878223	-3.054618	2.73648
C16	-3.155535	-2.968251	2.171415
C17	-3.293589	-2.262918	0.972229
C18	-2.204806	-1.801294	-2.190411
C19	-3.90465	-0.264179	-1.091272
C20	-4.353312	-3.595224	2.843926
C21	-0.676242	1.390144	2.755401
C22	-1.004315	2.135982	3.884986
C23	-1.27439	3.492397	3.721959
C24	-1.210746	4.050258	2.447607
C25	-0.879191	3.237769	1.357089
C26	-0.784151	3.753275	-0.037833
C27	-1.099033	5.070555	-0.392265
C28	-0.973546	5.461667	-1.723411
C29	-0.540729	4.534772	-2.668879
C30	-0.252626	3.240614	-2.237758
F1	2.204235	0.328852	2.18556
F2	4.320409	-0.010511	1.832794
F3	3.452147	1.944779	1.443392
F4	3.875959	0.0775	-2.281157

F5	4.077337	1.950309	-1.203303
F6	5.284672	0.255869	-0.626488
F7	-0.915804	-2.197922	-2.214741
F8	-2.468047	-1.214436	-3.371773
F9	-2.965743	-2.916239	-2.110644
F10	-4.219669	0.408308	0.037082
F11	-4.862765	-1.211386	-1.275413
F12	-4.019311	0.59238	-2.114929

13. Magnetic susceptibility measurements for 3.

The magnetic susceptibility of **3** is largely dependent on the drying time of the sample. Table S30 shows the room temperature solution $\chi_M T$ measured by Evans method as a function of the drying time, while Figure S28 shows the effect of the drying time on the temperature-dependent magnetic susceptibility plot collected. This strong correlation with the drying time is caused by the presence of solvent molecules in the crystal lattice. As a consequence, the drying time dependence of the magnetic susceptibility arises from a decrease in the molecular weight. When the molecular weight of the dry compound is used to obtain the molar magnetic susceptibility of samples that are not completely dry, the resulting values are lower than they would be if the correct molecular weight was used.

Table S30. Drying time dependence of the solution $\chi_M T$ measured by Evans method.[4]

Drying time (h)	$\chi_M T$ (cm^3 K mol^{-1})
0	3.94
4	4.33
6	4.53

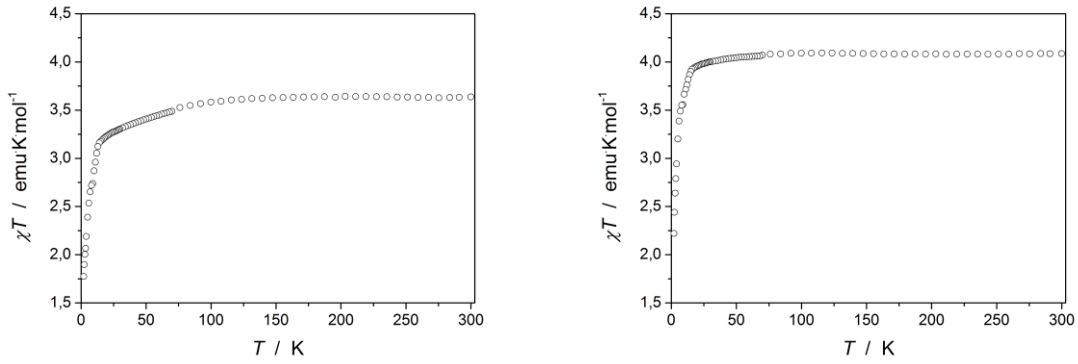

Figure S28. Effect of drying time on the temperature-dependent magnetic susceptibility plots for **3** in a 2000 G field. Increasing the drying time (from left to right) results in a higher room temperature $\chi_M T$ value.

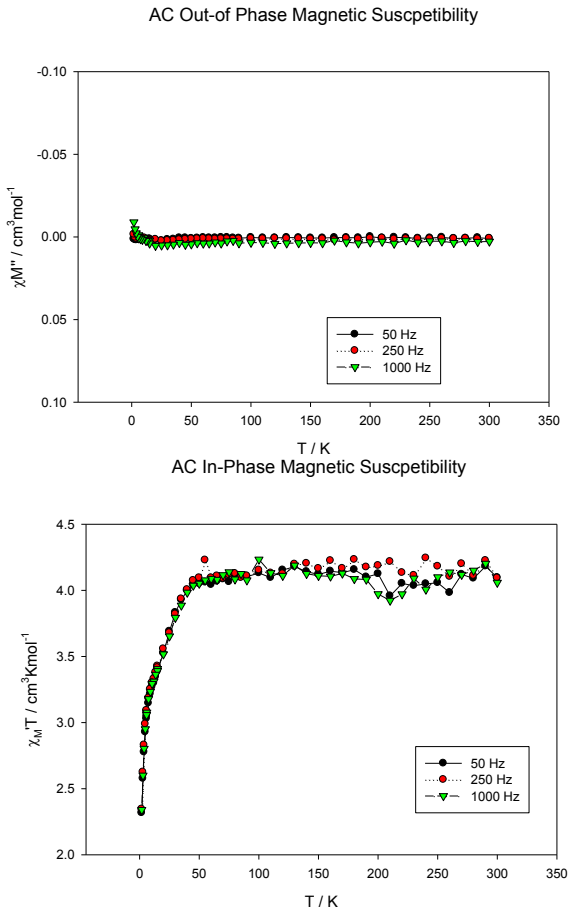

Figure S29. Temperature dependent AC out-of phase (top) and in-phase (bottom) magnetic susceptibility plot for **3**.

14. EPR spectroscopy and magnetometry measurements for 4 and 5.

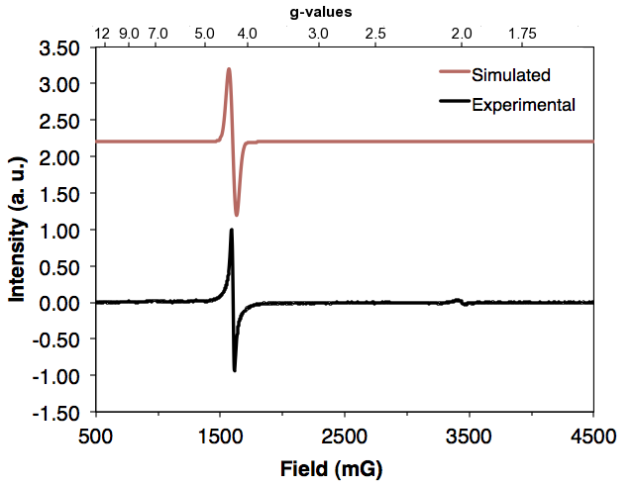

Figure S30. X-band EPR spectra of **4** collected as a toluene solution at room temperature and simulated with EasySpin[4] using the values of $S_1 = S_2 = 5/2$, $g_1 = g_2 = 2.00$, $D = 3.0$ cm^{-1}, and $E = 0.33\ D$.

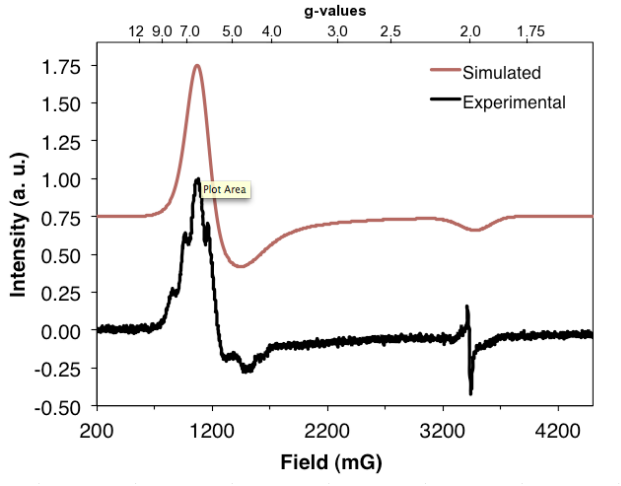

Figure S31. X-band EPR spectra of **5** collected as a toluene solution at room temperature and simulated with EasySpin[4] using the values of $S = 5/2$, $g_x = 1.90$, $g_y = 2.00$, $g_z = 1.97$, $D = 2.5$ cm^{-1}, and $E = 0.01\ D$.

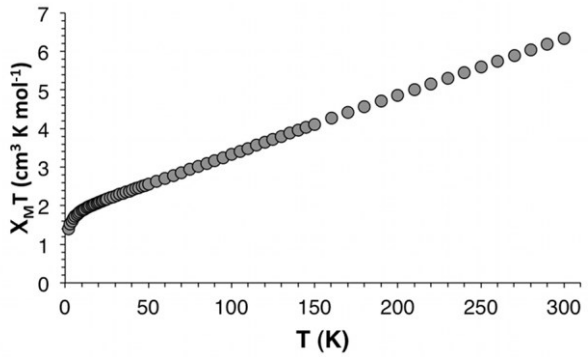

Figure S32. Temperature-dependent magnetic susceptibility times temperature plot for **4** in 100 G. The room temperature $\chi_M T$ value of 6.33 cm^3 K mol^{-1} is below the free-spins (two Fe(III) per formula unit) value of 8.75 cm^3 K mol^{-1}. The solution magnetic susceptibility is 7.93 cm^3 K mol^{-1}.[4]

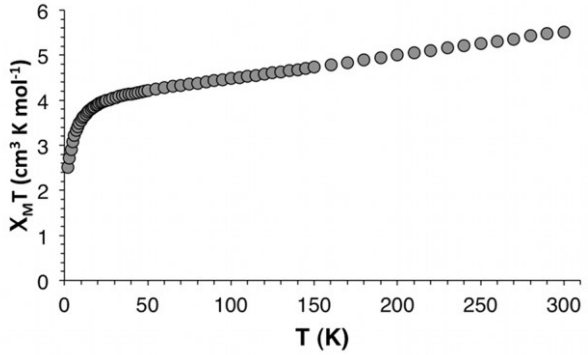

Figure S33. Temperature-dependent magnetic susceptibility times temperature plot for **5** in 100 G. The room temperature $\chi_M T$ value of 5.52 cm^3 K mol^{-1} is above the free-spin Fe(III) value of 4.38 cm^3 K mol^{-1}.

15. References.

(1) Becke, A. D., *J. Chem. Phys.* **1993,** *98*, 5648-5652.

(2) Lee, C.; Yang, W.; Parr, R. G., *Phys. Rev. B* **1988,** *37*, 785-789.

(3) Frisch, M. J.; Trucks, G. W.; Schlegel, H. B.; Scuseria, G. E.; Robb, M. A.; Cheeseman, J. R.; Scalmani, G.; Barone, V.; Mennucci, B.; Petersson, G. A.; Nakatsuji, H.; Caricato, M.; Li, X.; Hratchian, H. P.; Izmaylov, A. F.; Bloino, J.; Zheng, G.; Sonnenberg, J. L.; Hada, M.; Ehara, M.; Toyota, K.; Fukuda, R.; Hasegawa, J.; Ishida, M.; Nakajima, T.; Honda, Y.; Kitao, O.; Nakai, H.; Vreven, T.; Montgomery, J., J. A.; Peralta, J. E.; Ogliaro, F.; Bearpark, M.; Heyd, J. J.; Brothers, E.; Kudin, K. N.; Staroverov, V. N.; Keith, T.; Kobayashi, R.; Normand, J.; Raghavachari, K.; Rendell, A.; Burant, J. C.; Iyengar, S. S.; Tomasi, J.; Cossi, M.; Rega, N.; Millam, J. M.; Klene, M.; Knox, J. E.; Cross, J. B.; Bakken, V.; Adamo, C.; Jaramillo, J.; Gomperts, R.; Stratmann, R. E.; Yazyev, O.; Austin, A. J.; Cammi, R.; Pomelli, C.; Ochterski, J. W.; Martin, R. L.; Morokuma, K.; Zakrzewski, V. G.; Voth, G. A.; Salvador, P.; Dannenberg, J. J.; Dapprich, S.; Daniels, A. D.; Farkas, O.; Foresman, J. B.; Ortiz, J. V.; Cioslowski, J.; Fox, D. J. *Gaussian 09, Revision D.01*, Wallingford CT, 2013.

(4) Evans, D. F. *J. Chem. Soc.* **1959**, 2003.

(5) Stoll, S.; Schweiger, A. *J. Magn. Reson.* **2006**, *178*, 42.